RAIN EFFECTS ON ASCAT RETRIEVED WINDS: TOWARDS AN IMPROVED QUALITY CONTROL

Journal:	*Transactions on Geoscience and Remote Sensing*
Manuscript ID:	TGRS-2011-00472.R1
Manuscript Type:	Recent Advances in C-Band Scatterometery Special Issue
Date Submitted by the Author:	21-Sep-2011
Complete List of Authors:	Portabella, Marcos; UTM - CSIC, R&D Stoffelen, Ad; KNMI, Weather research Lin, Wenming; ICM - CSIC, Physical oceanography Turiel, Antonio; ICM - CSIC, Physical oceanography Verhoef, Anton; KNMI, Weather research Verspeek, Jeroen; KNMI, Weather research Ballabrera, Joaquim; UTM - CSIC, R&D
Keywords:	Remote sensing, Microwave measurements, Quality control, Geophysical inverse problems, Image processing

Answer to Reviewer #1

1. The main source of my concern is the fact that the only *validation source* that is used in the study are the ECMWF wind speeds. As the authors state by themselves throughout the paper, it is difficult to figure out who is actually to blame for certain observed problems: ASCAT, ECMWF or both. The authors try to do a lot of forth and back arguing, but I must admit, that after reading the manuscript the conclusion remains quite vague and unclear to me. A quantitative assessment of the rain impact is very difficult, as long as it not really understood if and how the ECMWF winds themselves are impacted by rain. In short, I believe the whole study of rain impact on ASCAT, which is an important one, would strongly benefit if an additional data source would be included for comparison. The best and least ambiguous one are **buoy wind speeds**. Even with using only 1 year of ASCAT data there should be plenty collocations to work with. That also would allow to make a better quantitative assessment, which is important.

Indeed, we agree that the buoy data information improves the analysis and the conclusions of the paper. We found very few and statistically insignificant quadruple collocations of ASCAT-ECMWF-buoy winds + TMI rain. However, we have built a 4.5-year (almost the entire ASCAT mission) quadruple collocation dataset of ASCAT-ECMWF-buoy winds + buoy rain information, which we believe provide statistically significant results that support our original conclusions. You'll find the details of the buoy work in sections 2 and 4.2.

2. I am having difficulty understanding Figure 5 showing the *vector RMS* between ASCAT and ECMWF. I suggest that the figure is redrawn or another figure is added that shows the RMS for the scalar wind speed differences and the wind direction differences separately. It would also be good to separate out bias and standard deviation rather than giving only the RMS. It is important to be able to separate the rain impact on scalar wind speed and direction. For example in case of QuikSCAT it is known that the rain impacts mainly the scalar wind speed, whereas wind direction is much less impacted beside for very high rain rates.

Indeed, the speed and direction differences analysis is helpful. In section 4.2, a figure is added (see Figure 10) to discuss the rain impact on ASCAT wind speed and direction components. Figures7, 8, and the new Figure 11 provide a good indication of the wind speed biases.

3. The question if ASCAT or ECMWF or both are contaminated by rain even for zero rain rate needs to be better investigated and clarified. The arguments provided in the manuscript are much too vague. One easy thing the authors could and should do in order to shed light on that, is to use the TMI wind speeds in their collocated data set. TMI does produce scalar wind speeds in rain free areas; they are good and have been validated against many sources to an accuracy of about 0.8 – 1.0 m/s. The authors can easily calculate the biases and standard deviations for TMI – ASCAT and TMI - ECMWF wind speed differences in their data sets. They can do that for observations that have zero rain rate and no adjacent rain and then for observations that have zero rain rate but rain in adjacent cells. (By the way, also SSMIS F16 is a good candidate for doing that, as it should collocate relatively well with ASCAT and it is not restricted to low latitudes. Of course it would be a different data set).

Regarding TMI wind information, it is known to be much affected by rain in adjacent cells. In a personal communication with Lucrezia Ricciardulli (Remote Sensing Systems), an expert in TMI processing, she said that when deriving their TMI wind GMF for dry conditions, the GMF shape would remarkably change when including no-rain data adjacent to rain cells in the fitting dataset. This is due to the high sensitivity of the TMI channels to rain. We believe, however, that ASCAT is much less sensitive to rain in adjacent cells, even though some rain contamination may be present due to the Hamming window processing. Variability of ocean roughness would be detectable with both TMI and ASCAT (if the former had less rain contamination). ECMWF winds are not affected by rain, but may rather lack wind variability in the proximity of wet convection due to lack of effective resolution. We sought confirmation of these points by independent buoy wind and rain data (see section 4.2).

4. Page 9, line 46 ff: How big is the effect of *downbursts and convergence* on wind speed speeds quantitatively? Have there been reliable studies done that could be cited? The presented argument is again too vague. That is one of those issues where using buoy wind speeds would be very helpful.

Mouche et al. (Scatterometer conference, Darmstadt, April 2011)show an example with large variability due to a downburst and relative cross-track wind component variation from -1 to +2 m/s (see figure below). In section 4.2, an attempt to quantify this effect with the limited number of ASCAT-ECMWF-buoy collocations is now incorporated (see for example, Table 2).

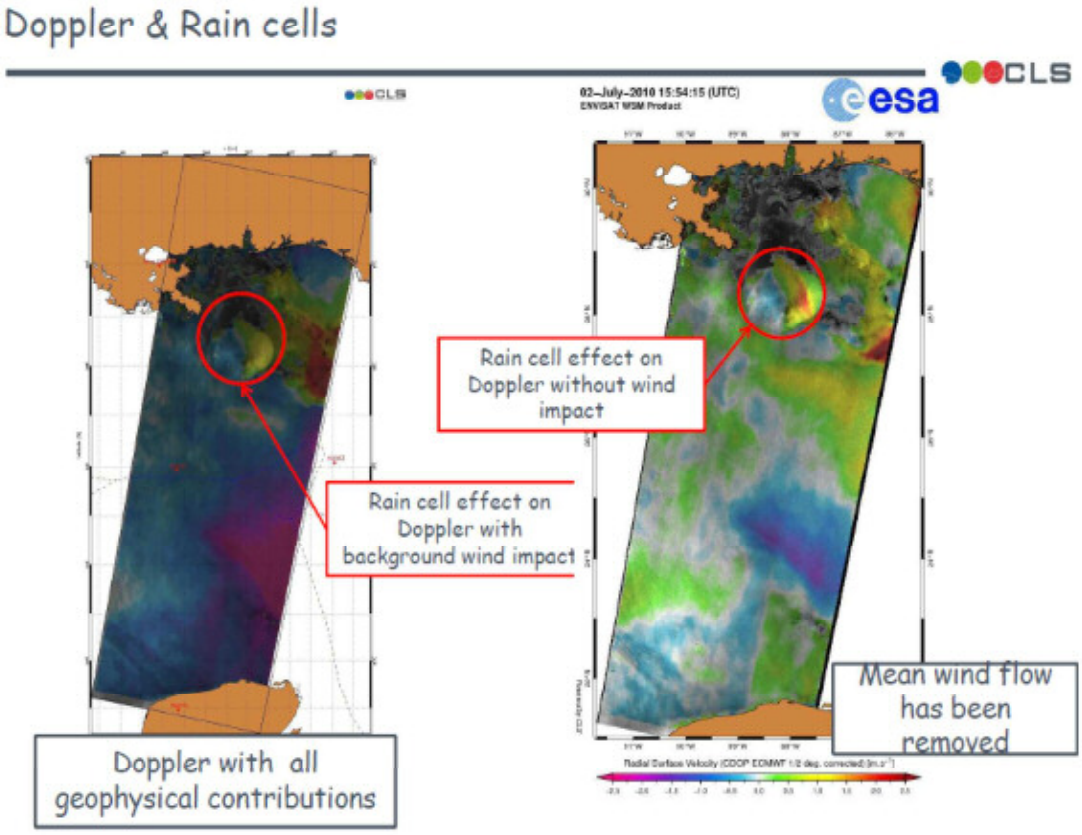

5. A general note: The authors present their results for different geographical regions. They might want to consider adding or substituting that with presenting the results for different wind speed regimes instead. The main driver that determines the wind speed algorithm degradation in rain are wind speed and rain rate. The geographic location is of course correlated with wind speed but it is not really the main driver.

We agree wind speed and rain are determining factors within each climate zone, but due to relatively low sensitivity to rain clouds, ASCAT winds appears sensitive to wind variability associated with rain too. The geographical locations chosen in this paper are correlated both with wind speed and wind variability, i.e., extratropical winds are more gusty than tropical ones. Moreover, rain columns in the tropics are much deeper and thus the downbursts much more intense. As such, we believe that these two different regions are quite complementary in terms of wind & rain conditions. Moreover, Figures7 and 8 provide insight on the relation between wind speed and rain regimes.

6. Page 11, line 48 ff: As the subject of the study is *Towards an Improved Quality Control*, I think it would be nice to have a figure or table that show explicitly results comparing MLE > 18 and MLE > 2.

As mentioned in section 4.1, lowering the MLE threshold to 2 does not have any impact whatsoever in the wind direction artefacts seen in Figure 9. As such, we see no point in

providing false alarm rates and probability of detection indicators since there is no trade-off between lowering the threshold and removing such artefacts. Moreover, the buoy analysis results (see new section 4.2) suggest that ECMWF wind directions are inaccurate under unstable and rainy conditions. In addition, they do not reveal wind direction accumulations in ASCAT winds. As such, buoy analysis may be very useful in further improving the ASCAT QC, provided that a larger collocation dataset is available. We plan to work on this topic in the near future.

7. Page 5, line 8 ff: It is somewhat mysterious why points outside the cone behave that much differently from points inside the cone. Do the authors have an explanation for that? The reference they cite has just recently been submitted.

In physical terms, triplets well outside the cone correspond to an anomalous anisotropic ocean surface associated with winds blowing at a constant speed and a very steady wind direction, while triplets well inside the cone correspond to an anomalous isotropic ocean surface associated with variable winds blowing at a varying speed and from different wind directions. In the latter case, the wind vector is less well determined.The corresponding reason for the different wind direction retrieval skill (and therefore wind vector skill) for triplets located far inside and far outside the cone surface is the following. Let's assume, for example, a true wind with a crosswind direction (relative to mid beam), which can be represented in the Figure below by a point at the bottom of the cross section. Take a measurement triplet ($\vec{z}_0$) inside the cone and close to the true wind direction and move it away from the surface. At a certain point, the triplet may lie closer to the opposite side of the cross section, i.e., the top part (upwind/downwind directions), therefore leading to a set of very wrong wind directions in the retrieval process. Another interesting effect is that when the triplet lies close to the centre of the cross section, the number of retrieved wind direction ambiguities increases from two (typical case for ASCAT) to four (not shown). Now, take the same crosswind triplet, but this time located outside the cone, and move it away from the surface. The triplet's closest distance to the cone will remain in the crosswind region, indicating that the wind direction skill is not much affected in this case. Moreover, the number of retrieved ambiguities remains the same, i.e., two (not shown). Similarly, non-perpendicular, i.e., sideways, noise contributions cause larger wind direction errors for triplets within the cone than for triplets outside the cone (not shown).

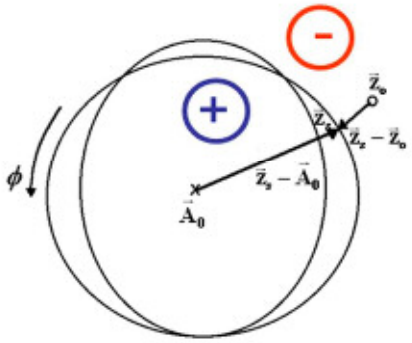

Schematic illustration of a cross section of the CMOD5n GMF. Note that $\vec{z}_s$ refers to a point on the cone surface as determined by inversion; $\vec{A}_0$ represents the major axis location at this cross section; and $\vec{z}_0$ represents the measurement triplet.

8. Page 3, line 23/24: Consider substituting the words *emitted* by *scattered* or *reflected*.

Done.

9. Page 14, line 16: Insert… many other WVC are not *rejected* ….

Done.

Answer to Reviewer #2

The authors attempt to address three questions 1) What is the impact of rain on ASCAT winds? 2) How well does the current ASCAT flagging scheme handle rain? And 3) How well would a new scheme involving Singularity Analysis work?

The primary focus appears to be on question 1. Question 2 is addressed quantitatively in terms of histograms, but the discussion is inadequate as it does not address specifics such as false alarm rates, missed detection rates, etc. Question 3 is only anecdotally addressed. The paper would flow better if the distraction of the SA method were left out entirely.

Indeed, the primary focus is on question 1. Question 2 is difficult to quantify in terms of false alarm rates, missed rates, etc., since there is no abundant, independent, and reliable wind dataset, representative of scatterometer scales, to use for validation purposes. Following both reviewers' suggestion, we have however now analysed buoy data (see sections 2 and 4.2).The latter indeed provide additional information on the problem. However, the collocation dataset is still limited for producing the already mentioned quantitative results.

Regarding question 3, we agree that it is not answered. However, we believe that since this is a Special Issue on C-band scatterometry, it is important to highlight new techniques that show potential to improve scatterometer processing. Moreover, with the inclusion of the buoy analysis, we believe that the goals of the paper are much clearer now.

I disagree somewhat with the authors' conclusions on Question 1. I agree that rain rates above 6 mm/hr adversely affect ASCAT retrievals, but from looking at the Figures 5 and 8, I would state that anything over 2-3 mm/hr also adversely affects ASCAT retrievals. I do not agree that low rain rate differences between ASCAT and ECMWF are solely due to ECMWF error. The marked increase (Fig 8) in the occurrence of 90, 180, 270 and 360 degree wind directions for 2-3 mm/hr cases over 0 mm/hr cases seems to me to be enough to show that 2-3 mm/hr rain significantly degrades ASCAT performance. See specific comments below for more details.

Indeed, rain may change ASCAT wind retrieval properties. The effect is well known and is caused by anomalous isotropic sea surface conditions. At some of the wind speeds and rain rates concerned, this may be caused by splash, but we believe that generally this is caused by increased wind variability in the proximity of rain, as now corroborated with the buoy verification (see section 4.2). However, the latter does not confirm the wind direction accumulations seen in Figure 9, but rather points to ECMWF

wind direction inaccuracies under rainy conditions. In future work we plan to further address this issue and improve scatterometer wind retrievals under conditions of wind variability.

I strongly suggest adding TAO buoy wind comparisons to the analysis. An extra data source would go a long way toward answering the question of when to attribute errors to ASCAT or ECMWF. This is an important question. If the authors are right, for low rain rates, ECMWF is flawed and ASCAT winds are preferable inputs for all scientific and operational use. If they are wrong, then ASCAT data may only be preferable to ECMWF for rain-free conditions. If the authors could use buoy data to conclusively answer this question, then the result would be a highly useful paper.

Indeed, we agree that the buoy data information improves the analysis and the conclusions of the paper. We found very few and statistically insignificant quadruple collocations of ASCAT-ECMWF-buoy winds + TMI rain. However, we have built a 4.5-year (almost the entire ASCAT mission) quadruple collocation dataset of ASCAT-ECMWF-buoy winds + buoy rain information, which we believe provides statistically significant results that support our original conclusions. As already mentioned, the reviewer will find the details of the buoy work in sections 2 and 4.2.

Page 5 line 23 expand AWDP acronym.
Page 5 line 23 "MLE>18.6 (accounting for the sign)." This is awkwardly phrased. I suppose this means MLE>+18.6. Right?
Page 7 top of page states that "two regions of interest with substantial collocations under rainy conditions" are outlined in Figure 2, but in the caption of figure 2 the outlined regions are not mentioned. Please correct this omission.

AWDP is already expanded in page 3, line 26. All other suggestions have been adopted in the manuscript.

Page 9 The authors claim that the increase in VRMS and biases for low rain rates may be due to ECMWF error. It also may be due to a greater than expected splash (scatter from rain drops impacting surface) effect. This effect has not been well-modeled, so the low expectation may bear no relationship to reality. I suggest comparing with TAO buoys in addition to ECMWF. If the TAO buoys and ASCAT agree against ECMWF then I would attribute the error to ECMWF. If the buoys and ECMWF agree against ASCAT, the splash effect is likely stronger than expected. Even if all three disagree with similar VRMS, bias comparisons may still shed light on the question.

As suggested by both reviewers, a thorough analysis using buoy data has been carried out and presented in section 4.2. Unfortunately, due to the limited amount of ASCAT-ECMWF-buoy collocations (see section 2), it is difficult to quantify the sea-surface rain

splashing effect on ASCAT. However, we found that our main conclusions, i.e., ECMWF does not well resolve rain-induced winds and ASCAT is impacted by rain splashing for significant rain rate, are corroborated with the buoy analysis results.

Page 10 bottom half: The authors claim the large VRMS vs. ECMWF for RR=0 in regions of high rain frequency is due to ECMWF poorly modeling these regions. An alternative explanation is that nearby rain may be contaminating the Hamming-filtered ASCAT backscatter data. I suggest attempting to reproduce these results using the box-filtered "coastal" ASCAT data product. Even then, care needs to be taken to exclude "rain-free" cells that have rain near enough (<50 km) to impact the measurements in the box. Buoy comparison would really help to resolve this issue. Admittedly buoy data is scarce, but it has excellent temporal sampling so triple TRMM/ASCAT/TAO buoy data does exist.

As already mentioned in this document and in the manuscript, we have collocations with buoy data. As such, we can draw some conclusions for WVCs in the vicinity of rain cells. As shown in section 4.2, ASCAT winds from category 3 (unstable conditions, with rain cells in the vicinity of the ASCAT WVC) do not show much of a rain splashing pattern. That is, in Figures 10, 11, and 12,ASCAT winds are unbiased w.r.t. buoy winds and in closer correspondence with buoys as compared with ECMWF winds).Moreover, the buoy/ECMWF wind time series (Figure 12) clearly show that ECMWF winds do not well resolve the wind flow in the vicinity of rain. We have evidence that the Hamming filtering will indeed somewhat spread the rain impact over ASCAT winds, but mostly in extreme cases where most of the surrounding WVCs are affected by rain and where the MLE>18. In cases where we process winds, it has been verified that the Hamming and box-filtered products have almost identical wind field characteristics. When a long box-filtered time series exist, verification of its QC against buoys as initiated here, should indeed be performed.

Page 10: The authors address the point above by saying ""some rain contamination of the ASCAT radar footprint may occur for TMI rain-free co-located WVCS, [but] this should be small." I disagree. It need not be small. Figure 6 shows that wind speeds can be substantially affected by large rain rates. A 3 m/s bias in wind speed can indicate a several dB bias in backscatter. Such a large effect may bias measurements significantly even if the effect is reduced by lower weighting. Since the Hamming filter weights are still quite high up to 100 km away from the wind vector cell, this problem is not insignificant.

See the answer to the previous point and the analysis in section 4.2.

Page 11: As the authors state Figure 8 shows that obvious directional artifacts creep into ASCAT winds even for low rain rates. This strengthens my argument that the VRMS and speed bias results determined for low rain rates need not be due to ECMWF error. Buoy comparisons are needed.

Same as previous point.

Figure 9: Gray color is referred to a "blue".

The "blue" refers to the colour of the wind arrows which have passed the QC.

RAIN EFFECTS ON ASCAT RETRIEVED WINDS: TOWARDS AN IMPROVED QUALITY CONTROL [1]

Marcos Portabella[1], Ad Stoffelen[2], Wenming Lin[3], Antonio Turiel[3], Anton Verhoef[2], Jeroen Verspeek[2], Joaquim Ballabrera[1]

[1]Unitat de Tecnologia Marina (UTM-CSIC), Pg. Marítim de la Barceloneta 37-49, 08003 Barcelona, Spain.

[2]Royal Netherlands Meteorological Institute (KNMI), Postbus 201, 3730 AE De Bilt, The Netherlands

[3]Institut de Ciències del Mar (ICM-CSIC), Pg. Marítim de la Barceloneta 37-49, 08003 Barcelona, Spain.

Phone: +34-932309500, Fax: +34-932309555

E-mail: portabella@cmima.csic.es

Abstract

The quality of the Ku-band scatterometer derived winds is known to be degraded by the presence of rain. Little work has been done in characterizing the impact of rain on C-band scatterometer winds, such as those from the Advanced Scatterometer (ASCAT) on board Metop-A. In this study, the rain impact on the ASCAT operational Level 2 quality control

[1] Revised manuscript submitted to the Special Issue on Recent Advances in C-band scatterometry, *IEEE Trans.*

(QC) and retrieved winds are investigated using the European Centre for Medium-range Weather Forecasts (ECMWF) model winds, the Tropical Rainfall Measuring Mission's (TRMM) Microwave Imager (TMI) rain data, and tropical buoy wind and precipitation data as reference. In contrast to Ku-band, it is shown that C-band is much less affected by direct rain effects, such as ocean splash, but effects of increased wind variability appear to dominate ASCAT wind retrieval. ECMWF winds do not well resolve the air flow under rainy conditions. ASCAT winds do, but also show artefacts in both the wind speed and the wind direction distributions for high rain rates. The operational QC proves to be effective in screening these artefacts, but at the expense of many valuable winds. An image processing method, known as the singularity analysis, is proposed in this study to complement the current QC and its potential is illustrated. QC at higher resolution is also expected to result in improved screening of high rain rates.

1 Introduction

The Metop-A satellite was launched on 19 October 2006 carrying, among other instruments, the Advanced Scatterometer (ASCAT). The latter is a real aperture, C band, vertically polarized radar with three fan beam antennas pointing to the left hand side of the sub-satellite track and three fan beam antennas pointing to the right hand side [1]. Scatterometers are known to provide accurate mesoscale (25-50 km resolution) sea surface wind field information used in a wide variety of applications, including Numerical Weather Prediction (NWP) data assimilation, nowcasting, and climate studies. The radar antenna geometry, the measurement noise, as well as the non-linearities in the relationship between the backscatter

measurements in a Wind Vector Cell (WVC) and the mean wind vector complicate the wind retrieval process. In addition, scatterometers are sensitive to geophysical phenomena other than WVC-mean wind, such as rain, local wind variability, confused sea state, and the radar footprint contamination by land and ice. These phenomena can distort the wind signal, leading to poor quality retrieved winds. As such, elimination of poor-quality data is a prerequisite for the successful use of scatterometer winds.

Rain is known to both attenuate and scatter the microwave signal [2]. Rain drops are small compared to radar wavelengths and cause Rayleigh scattering. As the rain rate increases, the radar sees less of the radiation scattered by the surface, and more of the radiation scattered by the rainy layer that becomes optically thicker due to volumetric Rayleigh scattering [3]. The higher the frequency of the radar, the larger is the impact of both effects (rain attenuation and scattering). In particular, Ku-band systems, such as the National Aeronautics and Space Administration (NASA) scatterometer (NSCAT) [4] onboard ADEOS, the SeaWinds scatterometers [5] onboard QuikSCAT and ADEOS-2, and the currently operating Indian scatterometer onboard Oceansat-2 (OSCAT), are significantly affected by rain. The European Remote Sensing Satellites (ERS-1 and ERS-2) scatterometer [6] and ASCAT operate at a relatively low frequency (5 GHz) and, as such, the mentioned effects are expected to be small. However, in addition to these effects, there is a "splashing" effect. The roughness of the sea surface is increased because of splashing due to rain drops. This increases the radar backscatter (σ^0) measured, which in turn will affect the quality of wind speed (positive bias due to σ^0 increase) and direction (loss of anisotropy in the backscatter signal) retrievals.

Another effect associated with heavy rain is increased wind variability. Convective rain cools the air below and reinforces downdraft near convective cells. These downdrafts often hit the ocean surface and cause outflow over the ocean, leading to variable wind speeds and

directions. Such variability within a WVC would increase the isotropy of the radar backscattering at the ocean surface, yielding lower quality wind retrievals.

Several methodologies have been proposed over the last 10-15 years to address the rain issue in scatterometry, notably for Ku-band systems. They can be grouped in the following three strategies: filtering rain-contaminated WVCs [7]-[9]; correcting for the rain-induced backscatter contribution [10]-[12]; and modelling both the rain- and the wind-induced backscatter with the objective of retrieving both parameters at the same time [13]-[14]. More recently, a neural network approach, which maps radar backscatter to wind in all weather conditions, is currently being used to reprocess QuikSCAT data [15]. For the operational Level 2 ASCAT Wind Data Processor (AWDP) [16], developed by the Royal Netherlands Meteorological Institute (KNMI) in the framework of the European Organization for the Exploitation of Meteorological Satellites (EUMETSAT) Numerical Weather Prediction (NWP) Satellite Application Facility (SAF), a Quality Control (QC) has been developed. This QC is based on the inversion residual or Maximum Likelihood Estimator (MLE) information [17]-[18], which can be interpreted as the closest distance of the ASCAT backscatter triplets (corresponding to the three antenna beams in each of the left and right swath) to the cone surface shown in Figure 1 [19]. For a given WVC position across the swath, the ASCAT-measured triplets are distributed around a well-defined "conical" surface and hence the signal largely depends on just two geophysical parameters, i.e., wind speed and direction. Such cone, the so-called CMOD5n Geophysical Model Function (GMF) [20], represents the best fit to the measured triplets and can in turn be used for Quality Control (QC) purposes.

In general, the triplets lie close to the cone surface (i.e., low MLE values), further validating the two-parameter (i.e., wind vector) GMF. As shown by several QC procedures developed for previous scatterometer missions [7], [17], [21], a large inconsistency with the GMF results

in a large MLE, which indicates geophysical conditions other than those modelled by the GMF, such as rain, local wind variability, confused sea state, or ice. As such, the MLE provides a good indication for the quality of the retrieved winds. Recent work [22] shows that for triplets located outside the cone surface, the quality of the retrieved winds is good regardless of their distance to the cone surface, i.e., MLE value. To account for this different behaviour inside and outside the cone surface, a sign is assigned to the MLE value, depending on whether the triplet is located inside (positive) or outside (negative) the cone surface. For more details on the MLE computation, see [22].

In the current version of the AWDP, any WVC with MLE > +18.6 is flagged as poor wind quality. Although the ASCAT QC has proved to be very effective in rejecting WVCs with poor wind quality while keeping those with good quality [22], it has not been specifically tested for rain effects.

On the other hand, an image processing technique, known as Singularity Analysis (SA), has been recently proposed as a complementary QC tool [23], in addition to the current ASCAT MLE-based QC. The SA uses multiscale wavelet projections to calculate the singularity exponents associated to a given signal. The singularity exponents are measures of the local regularity or irregularity of the signal and provide information about existing geophysical structures, characterized as singularity fronts [24]-[26], but also about any transition due to the presence of processing artefacts. Although further elaboration is needed, the method shows potential for complementing and therefore improving the current MLE-based QC.

In this paper, the rain impact on ASCAT derived winds as well as the effectiveness of the MLE- and SA-based QC techniques are tested. In Section 2, the different types of wind and rain data sources used in this study are presented. In Section 3, a thorough analysis of the rain impact on the ASCAT inversion residual or MLE is performed. The rain impact on the

ASCAT retrieved wind quality is analyzed in Section 4. The potential of the singularity analysis in detecting rain-induced artefacts in the ASCAT derived wind field is explored in Section 5. Finally, the concluding remarks and recommendations are discussed in Section 6.

2 Data

To study the effects of rain on both the quality of ASCAT retrieved winds and the performance of the MLE-based QC, two different collocation datasets are examined:

- The first dataset consists of one year (2008) of OSI SAF 25-km ASCAT Level 2 Binary Universal Format Representation (BUFR) data collocated with European Centre for Medium-range Weather Forecasts (ECMWF) winds and Tropical Rainfall Measuring Mission's (TRMM) Microwave Imager (TMI) rain data. The TMI data have been obtained from the Remote Sensing Systems web site (http://www.ssmi.com).

  Three ECMWF 3-hourly forecast winds (Analysis + 3h, +6h, and +9h) on a 62.5-km grid are interpolated both spatially and temporally to the ASCAT data acquisition location and time, respectively.

  The collocation criteria for TMI rain data are less than 30 minutes time and 0.25º spatial distance from the ASCAT measurement. Figure 2 shows the spatial distribution of the ASCAT-ECMWF-TMI collocations on a global map, both for rain free conditions (top) and for rain conditions (bottom). There is a total amount of about 6.4 million collocations, 5.9 million under rain-free conditions and 0.5 million for various rain conditions. When the collocation time is reduced to 15 minutes, the total number of collocations is reduced

to roughly 3 million. Note that the bottom panel highlights two regions of interest with substantial collocations under rainy conditions, i.e., the Pacific Inter Tropical Convergence Zone (ITCZ) and the Extratropical (North) Pacific area (see Section 4).

Also note that the collocations are confined between 40°S and 40°N, because of TRMM's low orbit inclination (35°). The Special Sensor Microwave Imager (SSM/I) onboard the Defense Meteorological Satellite Program (DMSP) satellites provide rain data at all latitudes. However, due to the difference in Equator crossing times between DMSP orbits and Metop-A orbit, virtually no collocations with ASCAT data are found for the mentioned time collocation criteria (either 15 or 30 minutes). Since this work requires small collocation errors, no SSM/I data are used.

- The second dataset used in this study consists of 4.5 years (March 2007- August 2011) of OSI SAF 25-km ASCAT Level 2 BUFR data collocated with ECMWF winds and tropical moored buoy wind and precipitation data. Only buoys equipped with a rain gauge are used in this dataset. By using the same collocation criteria as in the first dataset, a total amount of about 3400 collocations are obtained. Note that the reason for using this collocation dataset instead of collocation of all available buoy wind data with the ASCAT-ECMWF-TMI dataset is that the former yields three times more collocations than the latter.

  The tropical moored buoy data used correspond to the National Oceanic Atmospheric Administration (NOAA) TAO and PIRATA buoy arrays, which are located in the tropical Pacific and Atlantic Oceans, respectively, and the Research Moored Array for African-Asian-Australian Monsoon Analysis and Prediction (RAMA), which are located at the tropical Indian Ocean (see Figure 3). The data are available online at the following NOAA site: http://www.pmel.noaa.gov/. In this study, the buoy data distributed through the Global Telecommunication System (GTS) stream, quality controlled and archived at

ECMWF, and kindly provided by Jean-Raymond Bidlot are used instead. Details on the data quality control (QC) can be found in *Bidlot et al.* (2002). Note that, because of how the GTS data are encoded, the individual wind observations are only available to the closest m/s.

The buoy winds are measured hourly by averaging the wind speed and direction over 10 minutes. The real winds at a given anemometer height have then been converted to 10-meter equivalent neutral winds using the LKB model [27] in order to enable a good comparison with the 10-meter scatterometer and ECMWF winds. The buoy precipitation data are collocated with the buoy winds from the same position (i.e., the same buoy). Two different temporally-averaged rain rate parameters are computed, i.e., 2-hourly and daily.

3 Rain impact on ASCAT MLE

Figure 4 shows the histogram of MLE (i.e., distance-to-cone) values for different rain rate (RR) intervals. There is a clear bias of the MLE distributions towards positive MLE values (i.e., triplets located inside the cone) as RR increases. At RR= 0 mm/hr, the MLE distribution is almost symmetric with respect to the cone surface (almost the same distribution inside and outside the cone). In contrast, at RR above 6 mm/hr, most of the WVC triplets are located inside the cone (positive MLEs), with a substantial amount of triplets located very far away from the surface (large positive MLE values). This is an expected effect, since rain tends to produce a loss of anisotropy of the radar signal, therefore projecting the backscatter triplets inside the cone surface.

As mentioned in Section 1, the AWDP MLE-based QC does filter WVCs with MLE > 18.6. Negative MLEs (triplets outside the cone) are not filtered regardless of their magnitude (distance-to-cone). As the RR increases more WVCs with large positive MLEs are obtained and therefore filtered by QC. As shown in [22], a loss of anisotropy of the radar signal results in lower quality winds. As such, the loss of anisotropy due to rain is consistent with the AWDP QC.

Another interesting wind inversion parameter to examine is the number of ambiguities. Due to measurement noise and a highly non-linear GMF, scatterometer wind inversion does not yield a single wind solution but typically up to four wind solutions or ambiguities [28]. For ASCAT, the cone is a double-folded manifold, which usually implies dual ambiguity. Figure 5 shows the histogram of the number of ambiguities for different RR intervals. It is clear that for RR=0 mm/hr, most of the WVCs have only 2 ambiguities. For increasing RR, the number of ambiguities increases. As shown by Portabella et al. [22], ASCAT WVCs with poor quality retrieved winds usually have 3 or 4 wind ambiguities. Figure 5 therefore suggests that as RR increases the quality of the retrieved winds decreases. This result is in line with the MLE response to RR shown in Figure 5.

In summary, although MLE increases with RR, it is clear that with the current operational QC, many WVCs with MLE < 18.6 are affected by rain, even at high RR values (see Figure 4). One can further constrain the QC by reducing the MLE threshold. In doing so though, a significant amount of rain-free good quality WVCs will also be filtered out. As such, the MLE-based QC does not effectively screen rain for ASCAT. Nevertheless, the impact of rain on ASCAT wind retrieval quality needs to be assessed before drawing any conclusion on the MLE-based QC.

4 Rain impact on ASCAT winds

4.1 ASCAT-ECMWF-TMI analysis

To characterize the correlation between the RR and the quality of ASCAT retrieved winds, ECMWF winds are used as reference. Figure 6 shows the mean vector root-mean-square (VRMS) difference between ASCAT and ECMWF winds as a function of RR for different geographical locations. The solid line represents the results for the entire (global) collocation dataset. As expected, there is an increasing degradation of ASCAT derived winds for increasing rain rates. However, the substantial degradation within the first few mm/hr bins (the mean VRMS value is roughly doubled from RR=0 mm/hr to RR= 3mm/hr) is beyond the expected (small) rain impact in the C-band backscatter for such (low) rain rates. This increase in VRMS can alternatively be interpreted as an increase of ECMWF wind errors over rainy areas. Since the ASCAT TMI collocations are mostly within the tropics, ECMWF may be missing near-equatorial rain-related effects, such as downbursts and convergence.

Figure 7 shows the wind speed histogram of both ASCAT (a) and ECMWF (b) winds for different TMI-derived RR intervals. There is a clear positive wind speed shift in the ASCAT distributions for increasing RR which is not present in the ECMWF distributions. Although the (ASCAT) positive shift is consistent with the already mentioned rain splashing effect, the latter is expected to be small at such (low) rain rates. Moreover, downbursts and convergence are known to produce an increase in wind speed which is not well resolved by ECMWF (see rain-independent histograms in Figure 7b). However, for RR above 6 mm/hr, the difference between ASCAT and ECMWF wind distributions is well beyond the ECMWF uncertainty for rainy conditions, indicating a noticeable rain impact in the radar backscatter signal at such rain regimes.

As shown in Section 2, there are about 12 times more rain-free WVCs than rainy WVCs in the collocation dataset (see Figure 2). Moreover, the spatial distribution of rain-free and rainy datasets is remarkably different. This implies that the (true) wind distributions can indeed be substantially different for both datasets, therefore misleading the interpretation of the results in Figures 6 and 7. To ensure similar true wind distributions for rain-free and rainy conditions, the wind verification against ECMWF is performed in two different areas of interest with substantial collocations under rainy conditions, i.e., the ITCZ Pacific and the Extratropical Pacific areas (see Figure 2). Moreover, to match rain-free and rainy wind distributions a more restrictive selection procedure is used by only taking rain-free WVCs in the vicinity of rainy WVCs.

Going back to Figure 6, The VRMS scores are also shown for the ITCZ Pacific (dotted) and the Extratropical Pacific (dashed) areas. In comparison with the overall scores (solid), these two regions show a lower VRMS increase for low RR. In fact, VRMS scores are much higher in the Pacific areas for RR=0 mm/hr, notably in the Extratropics (dashed). Since ASCAT is known to perform well under rain-free conditions, this suggests that ECMWF does not well resolve the air flow in the vicinity of rainy areas, and therefore neither in rainy areas. Another explanation for the high VRMS in rain-free (according to TMI) WVCs neighbouring rainy WVCs is that in fact ASCAT winds may indeed be affected by rain. This is due to the time separation of up to 30 minutes allowed between ASCAT and TMI sensing time (see Section 2). In such period of time a neighbouring rainy cell may have moved several km, producing in turn a significant collocation error between ASCAT and TMI data. To reduce the collocation error, VRMS scores are recomputed with a new ASCAT-ECMWF-TMI collocated dataset using a reduced time separation of up to 15 minutes. Similar scores to those shown in Figure 6 are obtained. As such, although some rain contamination of the ASCAT radar footprint may occur for TMI rain-free collocated WVCs, this should be small. The results with the 15-min

dataset therefore reinforce the conclusion that ECMWF does not well resolve atmospheric dynamic features under rainy conditions, such as downdrafts.

Figure 8 shows the same as Figure 7 but for the ITCZ Pacific area. Note that, in contrast with Figure 7b, the ECMWF wind speed distributions (Figure 8b) are very similar for rainy and rain-free (near rain) WVCs, as expected. The ASCAT wind speed distributions (Figure 8a) though, show a similar increasing positive shift with increasing RR to that of Figure 7a.

Figure 9 shows the histogram of ASCAT (top) and ECMWF (bottom) wind direction relative to the ASCAT mid antenna beam for different RR values. The ASCAT wind direction distribution is very similar to that of ECMWF for rain-free WVCs, denoting good agreement between both wind sources. However, for rainy WVCs, the ASCAT distribution is substantially different from that of ECMWF. The former has clear artificial (non-geophysical) accumulations, especially at crosswind directions (90° and 270°), increasing with RR. The same wind direction artefacts are found for the two Pacific areas, as well as when reducing the collocation time to 15 minutes (not shown). This systematic effect in the wind direction retrievals is well known in scatterometry and has been reported by several authors (e.g., [29]-[31]. It is associated with scatterometer reduced wind direction skill. Portabella et al. [22] show that this effect usually occurs for ASCAT triplets located inside the cone and far from the surface. As such, the operational MLE-based QC generally shows good performance by detecting and filtering such artefacts. However, this is not the case under rain conditions. The same crosswind accumulations are found when repeating Figure 9 but only for WVCs with MLE<2, i.e., for triplets located near the cone surface.

Another interesting point is that the lack of ASCAT crosswind accumulations for rain-free WVCs in Figure 9a is also seen in the distributions of the Pacific areas (not shown). This further confirms that, in Figure 6 (dashed and dotted lines), ASCAT winds are not

(significantly) rain contaminated at the RR=0 mm/hr bin, and that the large VRMS at such bin is mostly due to ECMWF inaccuracies.

4.2 ASCAT-ECMWF-buoy analysis

To better disentangle the ASCAT and ECMWF rain effects, an independent wind source, such as buoy wind information, is required. Unfortunately, as mentioned in section 2, very few data are obtained from collocating all available buoy wind information with the ASCAT-ECMWF-TMI dataset. A 4.5 year (almost the entire ASCAT mission) collocated ASCAT-ECMWF-buoy winds + buoy rain dataset is used instead (see section 2). Two different RR parameters have been computed from buoy rain gauge time series: a 2-hourly RR and a daily average RR.

The 2-hourly RR has a very similar distribution to that of TMI rain (not shown). This is in line with the results found by [32]. _In particular, [32] finds that the maximum correlation between TMI and buoy rain gauge precipitation data is achieved by temporal averaging the buoy RR measurements around the satellite overpass time. The optimal temporal averaging window varies within 2-10 hours, depending on the spatial resolution of the TMI products. In particular, a 2-hour averaging is deduced to be optimal for spatial resolutions of 25-50 km, such as those of TMI and ASCAT. Therefore, the presence of significant 2-hourly RR should be a good indicator for rain contamination (surface splashing effect) of the ASCAT backscatter signal. Note however that rain-induced downdrafts are also expected.

The daily RR product is expected to effectively segregate rainy areas from dry areas, since atmospheric waves in the tropics are rather large-scale. In particular, for no significant daily RR, one expects no rain-related effects, i.e., no rain splashing or downdrafts effects.

Due to the lack of collocations, a detailed analysis as a function of RR values, as performed in section 4.1, cannot be done. A simple analysis using a combination of the two RR products

(i.e., 2-hourly and daily) and two different RR intervals, i.e., RR < 0.1 mm/hr and RR > 0.1 mm/hr, is carried out. Table 1 provides the number of collocations for the four possible combinations, i.e., categories C1-C4. Note that the results for C2 will not be shown since they lack statistical significance (very few amount of collocations). The results are however in line with the results in C1. This is expected since C2 presents low 2-hourly RR values (all below 1.5 mm/hr), further confirming that for daily RR < 0.1 mm/hr (C1+C2), the winds mostly correspond to dry stable atmospheric conditions. In contrast, categories C3 and C4 mostly correspond to rainy and unstable conditions. The main difference between these two categories is that C3 does not likely show local (at satellite overpass) rain conditions. As such, mainly rain-induced downdrafts are expected in C3, while both rain-induced downdrafts and local rain (splashing effect) are expected in C4.

In contrast with the dataset used in section 4.1, the ASCAT-ECMWF-buoy dataset contains three different wind sources. As such, a triple collocation analysis, as performed with a similar dataset by [33], can be performed in order to calibrate two winds sources (ASCAT and ECMWF) to a reference source (buoy). The calibration is carried out for “dry” winds only (i.e., C1, or likewise, C1 + C2) since the triple collocation analysis does not work well when mixing very different wind variability regimes (such as those from “dry” and “wet” winds). Moreover, as seen in Table 1, over rainy areas, there is little amount of collocations and therefore no statistically significant results are expected. Also important, by calibrating only in “dry” wind conditions, any bias in ASCAT or ECMWF winds (w.r.t. buoy winds) due to rain effects becomes more evident.

Figure 10 shows the scatter plots of ASCAT versus buoy winds (left) and ECMWF versus buoy winds (right) for wind speed (top) and wind direction (bottom) in C3. The left plots clearly present less scatter along the diagonal than the right plots, showing better agreement of

ASCAT winds w.r.t. buoy winds than ECMWF w.r.t. the buoys. This is confirmed by both the correlation and the RMS scores (see legend in Figure 10). However, since the number of collocations is small, the wind direction scores are very much influenced by a few outliers. By filtering these outliers, the RMS scores are reduced significantly, notably those of the ASCAT versus buoy wind directions (see Table 2). The scatter plots for C4 show a similar pattern than those of C3 (not shown). The effect of outliers in ASCAT statistics is even more exaggerated (see Table 2).

Interestingly, ASCAT wind directions do not show accumulations w.r.t. buoy wind directions (see Figure 10c). In contrast, ECMWF wind directions seem to accumulate around 90° and lack around 180° and 360° w.r.t. buoys (see Figure 10d). These wind direction patterns are even more pronounced in C4 scatter plots (not shown), suggesting that ECMWF wind directions are inaccurate under rain conditions.

Table 2 shows the VRMS difference between ASCAT and buoy winds (first column) and ECMWF and buoy winds (second column) for categories C1, C3, and C4. In general, ASCAT winds are in better agreement with buoy winds than those of ECMWF, indicating that ASCAT resolves smaller scales than ECMWF. In unstable (high wind variability) conditions (e.g., C3), area-mean winds (ASCAT and ECMWF) tend to differ more (larger VRMS) from point measurements (buoys) than in stable (low wind variability) conditions (C1). In C3, where the presence of rain-induced downdrafts is likely, ASCAT winds are clearly in better agreement with buoy winds than ECMWF. In C4, the VRMS scores are higher than in C3. Although ASCAT is still in better agreement with buoys than ECMWF, the difference in VRMS is smaller. This suggests a possible influence of the rain splashing effect in the ASCAT retrieval quality.

Figure 11 shows the wind speed distribution of the three wind sources for C3 (left panel) and C4 (right panel). In C3, the distributions are quite similar, notably buoy and ASCAT ones. However, in C4, the ASCAT distribution presents a positive shift with respect to the buoy distribution. This shift is similar to the one discussed in section 4.1, suggesting a noticeable impact of the rain splashing effect on the ASCAT retrieved winds.

Figure 12 shows two different buoy wind and rain time series, together with the collocated ECMWF forecasts for the period of ±24 hours of the ASCAT satellite overpass time. The first case shows an important rain event with its associated high wind variability pattern, including downdrafts. It is clear that ECMWF does not resolve such high resolution wind pattern, since it varies rather smoothly over this period. The second case shows again a case of high wind variability. Although no significant rain was recorded by the buoy, the downdraft-like wind pattern suggests the presence of rain cells in the vicinity. Again, the ECMWF wind pattern is rather smooth. In contrast, ASCAT is well resolving these high wind variability cases, as indicated by its good agreement with the collocated buoy wind (at the satellite overpass time).

In summary, small-scale wind variability appears to increase with rain occurrence. ECMWF does not well resolve the air flow near rain and is rather smooth. ASCAT winds are much better here, but show some systematic effects in the wind direction distributions when compared with ECMWF. The buoy analysis however reveals systematic effects in ECMWF wind directions rather than in ASCAT wind directions under rainy conditions. An increase in ASCAT wind speed bias in tropical rain may be due to splash effects. The MLE-based QC can detect and filter such rain effects, but possibly with rather low probability of detection and/or high false-alarm rate. An alternative method may therefore be useful to complement the current QC.

5 Singularity analysis

Singularity Analysis (SA) refers to any technique capable of evaluating the local singularity exponents of a given function around each one of its points. The concept of singularity exponent extends that of differentiability to a continuous range of cases, across which the regular character of the function can steadily vary. Singularity exponents also allow characterizing non-regular behaviours such as discontinuities and even actual divergences of the function to infinity.

To properly assess the local singularity exponent of a signal θ at the point **x** and scale r, noise, discretization effects, and long-range correlations need to be filtered by means of wavelet projections, namely

$$T_\psi \theta(\mathbf{x}, r) \equiv \int dx' \theta(\mathbf{x}') \frac{1}{r^2} \psi\left(\frac{\mathbf{x}-\mathbf{x}'}{r}\right) = \alpha(\mathbf{x}) r^{h(\mathbf{x})} + o\left(r^{h(\mathbf{x})}\right) \quad (1)$$

where the local exponents h(**x**) are obtained by a log-log linear regression of the last expression using a particularly well adapted wavelet. Something interesting about the formula above is that all the dependence in the scale parameter is a power law, which means that what characterizes the regularity or irregularity of a function is a scale-invariant quantity, the singularity exponent h(**x**). This in particular means that singularity exponents can be evaluated at any resolution, and also that they are dimensionless quantities which are hence unaffected by changes in the amplitude of the modulating signal. It has been shown that the wavelet projections of the modulus of the gradient of the signal θ allow characterizing the local singularity exponents with good spatial resolution [24]-[25].

Singularity analysis is a powerful image processing technique because it is strongly linked to the physics of the underlying fluid. As a consequence of the onset of turbulence in geophysical flows, any active or passive scalar in the ocean or the atmosphere is structured around singularity fronts, that is, the places at which singularity exponents take the minimum (typically negative) values. The singularity fronts determine the boundaries of the domains at which the flow changes its behaviour and hence can be identified with the main currents, as shown in repeated experiences with ocean surface image analysis (see Turiel et al. [26] and references therein).

When analyzing operational data such as ASCAT wind data, other singularity fronts are induced. This is mainly due to the fact that singularity analysis is normally applied to bi-dimensional maps of a given variable which is submitted to a process taking place in three dimensions. So that, convergence and divergence areas associated at circulation cell boundaries will show up as singularity fronts in ASCAT-derived maps, because they represent actual separation between two flow regimes as observed by the satellite. However, other effects not related to wind circulation induce spurious singularity fronts. For instance, any error in the determination of the wind speed or direction of the wind vector leads to marked singularity fronts, as analyzed in Turiel et al. [23]. In this Section, we are especially interested in observing this kind of effect when the source of the ill-determined wind vector is the presence of heavy rain in the ASCAT WVC.

Test case

Figure 13 shows an ASCAT retrieved wind field with TMI collocated rain rate values superimposed. Note that ASCAT QC rejects some of the WVCs under heavy rain (see red arrows around 6°N and 157°E), but many other WVCs with heavy rain are not rejected (see

central part of the wind field). The latter are in some occasions spatially inconsistent as denoted by their patchiness, but in other cases TMI heavy rain appears in areas with seemingly spatially consistent ASCAT winds. As discussed in Section 4, a more constrained QC (lower MLE threshold) may not be effective in filtering the wind artefacts.

Figure 14 shows a singularity map corresponding to the ASCAT wind field shown in Figure 13. The map is constructed as the minimum exponents of the singularity maps associated to the zonal (U) and the meridional (V) wind components, which were processed as scalar independently (see Turiel et al. [23] for further details). As shown in Figure 14, the presence of heavy rain bands (see pink- and red-filled circles in Figure 13) induce clear spurious singularity fronts, i.e., the places at which the value of singularity exponents is minimum (see bright lines in Figure 14). Also note that the values of singularity exponents all over the rain affected area are significantly smaller (whiter) than those outside the rainy area. The presence of rain decreases the signal-to-noise ratio of the radar backscatter. In turn, the ASCAT derived wind field over rainy areas seems to show less regularity than in nominal rain-free conditions, and hence lower singularity exponent values. Further analysis is required to confirm this effect.

In summary, although separating rain-induced singularity fronts from wind-induced ones is far from trivial, SA shows potential to assess the quality of the scatterometer retrieved wind fields.

6 Conclusions

The ASCAT level2 wind QC method, based on the inversion residual or MLE, is generally very useful in discriminating good wind quality WVCs from poor quality WVCs. In this paper, the effectiveness of the MLE-based QC is assessed for rain conditions. Although some correlation between the MLE value and the RR is found, the operational QC proves to be little effective in rain screening, i.e., by maximizing heavy-rain-contaminated WVC filtering, a substantial amount of rain-free good quality WVCs are inevitably filtered too. However, the effect of rain appears mainly in increasing the wind variability near the surface and, unlike for Ku-band scatterometers, RR itself does not appear clearly as a limiting factor in ASCAT wind quality.

To assess the impact of rain in the ASCAT wind retrieval quality, ECMWF winds are used as reference. It turns out that ECMWF does not well resolve the air flow under rain conditions. ASCAT winds however, show systematic effects in wind speed and direction distributions as a function of RR, which can be attributed to rain-induced wind-related effects, such as downbursts and/or convergence, but possibly also to splash effects for heavy rain. These systematic effects lead to degraded ASCAT wind quality, most notable for RR above 6 mm/hr. These results are corroborated with an independent buoy wind and rain dataset. Moreover, the buoy analysis reveals inaccuracies and systematic effects in ECMWF wind directions rather than in ASCAT wind directions under rainy conditions. However, the collocated buoy dataset is rather limited. Further analysis on the ASCAT wind speed and direction artefacts will be carried out provided that a larger buoy (wind and rain) dataset

becomes available. In addition, other independent and reliable data sources will also be explored.

An alternative method, based on singularity analysis, is proposed to complement the ASCAT operational QC. The method is tested here for a heavy rain case. The ASCAT singularity map identifies the main streamlines of the air flow. The presence of heavy rain induces clear spurious singularity fronts. Although separating rain-induced singularity fronts from wind-induced ones is challenging, preliminary results show the technique's potential to assess the quality of the scatterometer retrieved wind fields.

To contribute to the current ASCAT operational QC, further analysis is required. Future work will focus on analysing the relation between singularity fronts, for the ASCAT wind vector and each wind component (i.e., U, V, speed and direction) separately, and all geophysical phenomena which affect the radar backscatter signal, including rain, local wind variability, confused sea state, etc.

Both the MLE QC-based and the singularity analysis methods are expected to be more effective when applied on higher-resolution ASCAT products, i.e., 12.5-km and coastal products (see OSI SAF product at http:www.knmi.nl/scatterometer/). On the one hand, ASCAT is expected to better resolve higher resolution wind phenomena (e.g., convergence and downbursts); on the other hand, the rain splashing signal, being patchy and intermittent, is expected to become more evident at smaller ASCAT footprints. As such, we proceed to extend this study to the ASCAT high-resolution products.

Acknowledgments

The work has been funded under the EUMETSAT Ocean and Sea Ice (OSI) Satellite Application Facility (SAF) and its Associated Scientist program (project reference CDOP-SG06-VS03). The ASCAT level 1b data are provided by EUMETSAT. The software used in this work has been developed through the EUMETSAT Numerical Weather Prediction SAF. The ECMWF data are retrieved from the ECMWF MARS archive. The TMI data are available from the web site of Remote Sensing Systems (http://www.ssmi.com/). We thank Jean-Raymond Bidlot and ECMWF for providing the GTS buoy wind dataset (already quality controlled). The buoy rain data have been obtained from http://www.pmel.noaa.gov/.

References

[1] Figa-Saldana, J., Wilson, J.J.W., Attema, E., Gelsthorpe, R., Drinkwater, M.R., and Stoffelen, A., "The advanced scatterometer (ASCAT) on Metop: a follow-on for European scatterometers," *Can. Jour. of Rem. Sens.*, vol. 28, no. 3, 2002.

[2] Van De Hulst, H.C., "Light Scattering by small particles," *John Wiley and Sons*, New York, pp. 428, 1957.

[3] Boukabara, S.A., Hoffman, R.N., and Grassotti, C., "Atmospheric Compensation and Heavy Rain Detection for SeaWinds Using AMSR," *Atmospheric Environmental Research Inc.*, 131 Hartwell Ave., Lexington, Massachussets (USA), 2000.

[4] Naderi, F. M., Freilich, M. H., and Long, D. G., "Spaceborne radar measurement of wind velocity over the ocean: an overview of the NSCAT scatterometer system," *Proc. IEEE*, vol. 79, pp. 850-866, 1991.

[5] Spencer, M. W., Wu, C., and Long, D. G., "Tradeoffs in the design of a scapceborne scanning pencil beam scatterometer: application to SeaWinds," *IEEE Trans. on Geoscience and Rem. Sens.*, vol. 35(1), pp. 115-126, 1997.

[6] Attema, E. P. W., "The active microwave instrument on board the ERS-1 satellite," *Proc. IEEE*, vol. 79, pp. 791-799, 1991.

[7] Figa, J., and Stoffelen, A., "On the assimilation of Ku-band scatterometer winds for weather analysis and forecasting", *IEEE Trans. on Geoscience and Rem. Sens*., vol. 38 (4), pp. 1893-1902, 2000.

[8] Huddleston, J.N., and Stiles, B.W., "A Multi-dimensional Histogram Technique for Flagging Rain Contamination on QuikSCAT," Proc. of IEEE International Geoscience and Remote Sensing Symposium, Vol. 3, Honolulu (USA), IEEE, pp. 1232-1234, 2000.

[9] Portabella, M., and Stoffelen, A., "A comparison of KNMI quality control and JPL rain flag for SeaWinds," *Can. Jour. of Rem. Sens.,* vol. 28 (3), pp. 424-430, 2002.

[10] Stiles, B. W., and S. H. Yueh, "Impact of rain on spaceborne ku-band wind scatterometer data," *IEEE Transactions on Geoscience and Remote Sensing*, vol 40, no. 9, pp. 1973-1983, 2002.

[11] Hilburn, K. A., F. J. Wentz, D. K. Smith and P. D. Ashcroft, "Correcting active scatterometer data for the effects of rain using passive microwave data," *Journal of Applied Meteorology and Climatology*, 45, 382-398, 2006.

[12] Weissman, D.E. and M.A. Bourassa, "Measurements of the effect of rain-induced sea surface roughness on the QuikSCAT scatterometer radar cross section," *IEEE Transactions on Geoscience and Remote Sensing*, vol. 46, no. 10, pp. 2882-2894, 2008

[13] Draper, D.W. and D.G. Long, "Simultaneous wind and rain retrieval using seawinds data," *IEEE Transactions on Geoscience and Remote Sensing*, vol. 42, no. 7, pp. 1411-1423, 2004.

[14] Nie , C and D.G. Long, "A C-Band scatterometer simultaneous wind/rain retrieval method," *IEEE Transactions on Geoscience and Remote Sensing*, vol. 46, no. 11, pp. 3618-3632, 2008.

[15] Stiles, B.W, and Scott Dunbar, S., "A Neural Network Technique for Improving the Accuracy of Scatterometer Winds in Rainy Conditions," *IEEE Transactions on Geoscience and Remote Sensing*, vol. 48, no. 8, pp 3114-3122, 2010.

[16] Verhoef, A., J. Vogelzang, J. Verspeek and A. Stoffelen, "AWDP User Manual and Reference Guide," *NWPSAF-KN-UD-005*, version 2.0, EUMETSAT, 2010.

[17] Stoffelen, A., and Anderson, D., "Scatterometer data interpretation: measurement space and inversion," *J. Atmos. and Oceanic Technol.*, vol. 14(6), 1298-1313, 1997.

[18] Portabella, M., and Stoffelen, A., "Characterization of residual information for SeaWinds quality control," *IEEE Trans. Geosci. Rem. Sens.*, vol. 130, no. 596, pp. 127-152, 2002.

[19] Verspeek, J., Stoffelen, A., Portabella, M., Bonekamp, H., Anderson, C., and Figa Saldaña, J., "Validation and calibration of ASCAT data using ocean backscatter and CMOD5.n," *IEEE Trans. Geosci. Rem. Sens.*, doi:10.1109/TGRS.2009.2027896, 48 (1), pp. 386-395, 2010.

[20] Hersbach, H., A. Stoffelen, and S. de Haan, "The improved C-band ocean geophysical model function: CMOD-5," *J. Geophys. Res.*, 112, C03006, doi:10.1029/2006JC003743, 2007.

[21] Portabella, M., and Stoffelen, A., "Rain detection and quality control of SeaWinds," *J. Atm. and Ocean Techn*., vol. 18, no. 7, pp. 1171-1183, 2001.

[22] Portabella, M., Stoffelen, A., Verhoef, A., and Verspeek, J., "A new method for improving scatterometer wind quality control," submitted to *IEEE Geosci. Rem. Sens. Lett.*, June 2011.

[23] Turiel et al., "Quality control of ASCAT wind vector maps through singularity analysis," submitted to *Geophysical Research Letters*, June 2011.

[24] Isern-Fonanet, J., A. Turiel, E. Garcia-Ladona, and J.Font, "Microcanonical Multifractal Formalism: application to the estimation of ocean surface velocities," *J. Geophys. Res. – Oceans*, # C05{0}24, 2007.

[25] Turiel A., J. Sole, V. Nieves, J. Ballabrera-Poy, and E. Garcia-Ladona, "Tracking oceanic currents by singularity analysis of Micro-Wave Sea Surface Temperature images," *Remote Sensing of Environment,* vol. 112, pp. 2246-2260, 2008.

[26] Turiel A., V. Nieves, E. Garcia-Ladona, J. Font, M.-H. Rio, and G. Larnicol, "The multifractal structure of satellite temperature images can be used to obtain global maps of ocean currents," *Ocean Science*, vol. 5, pp. 447-460, 2009.

[27] Liu, W. T., K. B. Katsaros, and J. A. Businger, "Bulk parameterization of air-sea exchanges of heat and water vapor including the molecular constraints in the interface," *J. Atmos. Sci.*, vol. 36, 1979.

[28] Cornford, D., Csató, L., Evans, D. J., and Opper, M., "Baysian analysis of the scatterometer wind retrieval inverse problems: some new approaches," *J. R. Statist. Soc. B,* vol. 66, no. 3, pp. 609-626, 2004.

[29] Ebuchi, N., and Graber, H. C., "Directivity of wind vectors derived from the ERS-1/AMI scatterometer," *J. Geophys. Res.*, vol. 103(C4), pp. 7787-7798, 1998.

[30] Ebuchi, N., "Statistical distribution of wind speeds and directions globally observed by NSCAT," *J. Geophys. Res*., vol. 104(C5), pp. 11393-11404, 1999.

[31] Stoffelen, A., and Portabella, M., "On Bayesian scatterometer wind inversion," *IEEE Trans. Geosci. Rem. Sens*., vol. 44, no. 6, doi:10.1109/TGRS.2005.862502, pp. 1523-1533, 2006.

[32] Bowman, K.P., "Comparison of TRMM precipitation retrievals with rain gauge data from ocean buoys," *J. Clim.*, vo. 18, pp. 178-190, 2004.

[33] Vogelzang, J., Stoffelen, A. Verhoef, A., and J. Figa-Saldana, "On the quality of high-resolution scatterometer winds," *J. Geophys. Res.*, doi:10.1029/2010JC006640, in press 2011.

List of Tables and Figures

Fig. 4. MLE histogram for different rain rate (RR) intervals. Note that every coloured line corresponds to a different RR interval (see legend). The number of WVCs for each histogram is also provided in the legend.

Fig. 5. Number of ASCAT retrieved wind solutions (ambiguities) for different rain rate (RR) intervals (see legend).

Fig. 6. Mean vector root-mean-square (VRMS) difference between ASCAT and ECMWF winds (thick lines) and percentage of data (thin lines) as a function of TMI rain rate (bins of 1 mm/hr), for three different geographical regions: global (solid), the ITCZ Pacific region (dotted) and the Extratropical Pacific (dashed).

Fig. 7. Global wind speed histograms of both ASCAT (a) and ECMWF (b) winds for different TMI-derived RR intervals (see legend).

Fig. 8. Same as Fig. 7 but for the ITCZ Pacific region.

Fig. 9. Histogram of ASCAT (top) and ECMWF (bottom) wind direction relative to the ASCAT mid antenna beam (e.g., 0° corresponds to wind blowing towards the mid beam), for different RR intervals (see legend). Note that only WVCs with retrieved wind speed above 4 m/s are used.

Fig 10. Scatter plots of ASCAT versus buoy (left) and ECMWF versus buoy (right) for wind speed (top) and wind direction (bottom) on rainy days, but without rain within an hour of the ASCAT overpass [C3]. Note that only buoy winds above 4 m/s are used in the wind direction plots. The legend shows the correlation coefficient (CC), the standard deviation (SD) and the RMS difference.

Fig. 11. Histograms of buoy (solid), ASCAT (dotted) and ECMWF (dashed) wind speeds for C3 (a) and C4 (b). Due to the small number of collocations, the binning is set to 2 m/s.

Fig. 12. Time series of buoy winds and rain, and ECMWF wind forecasts for the period of ±24 hours of the ASCAT satellite overpass (see legend). The black circle represents the ASCAT retrieved wind speed. The first time series (a) corresponds to buoy 52003 [8°S, 165°E] and is centered on August 10 2007 at 22:00 UTC. The second time series (b) corresponds to buoy 52007 [5°N, 165°E] and is centered on July 5 2007 at 10:00 UTC.

Fig. 13. Map of collocated ASCAT-TMI data. ASCAT wind arrows, where blue corresponds to QC-accepted WVCs and yellow/orange to QC-rejected WVCs. The coloured areas superimposed correspond to different TMI rain rates (see legend). The acquisition date was October 14 2008 at 22:45 UTC.

Fig. 14. Singularity map of the ASCAT retrieved wind field shown in Fig. 9. The map is constructed as the minimum exponents of the singularity maps associated to the U and V wind components.

Illustrations

Table 1. Number of ASCAT-ECMWF-buoy collocations per rain category

	2h-Rain<0.1mm/hr	2h-Rain>=0.1mm/hr
1D-Rain<0.1mm/hr	2650 [C1]	59 [C2]
1D-Rain>=0.1mm/hr	506 [C3]	198 [C4]

Table 2. VRMS difference between ASCAT and buoy winds (first column) and between ECMWF and buoy winds (second column). In parenthesis, the same VRMS scores after filtering (3-sigma QC) 46, 12, and 15 outliers in C1, C3, and C4, respectively. A 3-sigma filtering has been applied, where sigma is 1.5 m/s in both u and v components.

	ASCAT – Buoy (m/s)	ECMWF – Buoy (m/s)
C1	1.78 (1.57)	2.29 (2.16)
C3	2.74 (2.41)	3.54 (3.34)
C4	4.26 (3.45)	4.34 (4.00)

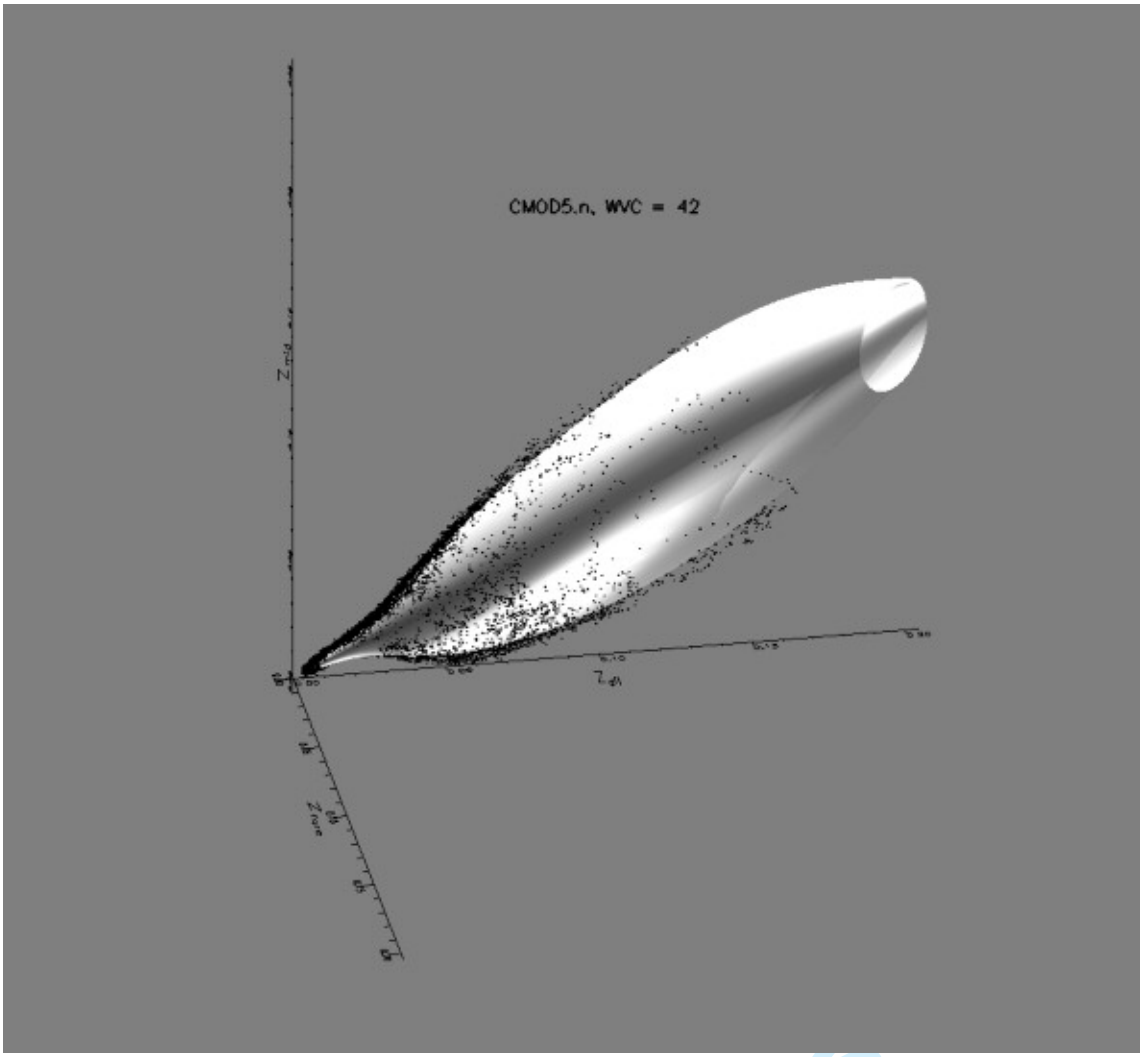

Fig. 1. Visualization of the CMOD5n GMF (grey surface) and the ASCAT triplets (black dots) in 3D measurement space, for ASCAT Wind Vector Cell (WVC) number 42. The axes represent the fore-, aft-, and mid-beam backscatter in z-space, i.e., (z_{fore}, z_{aft}, z_{mid}) where $z=(\sigma^\circ)^{0.625}$. Figure adopted from Figure 1 in Verspeek et al. [19].

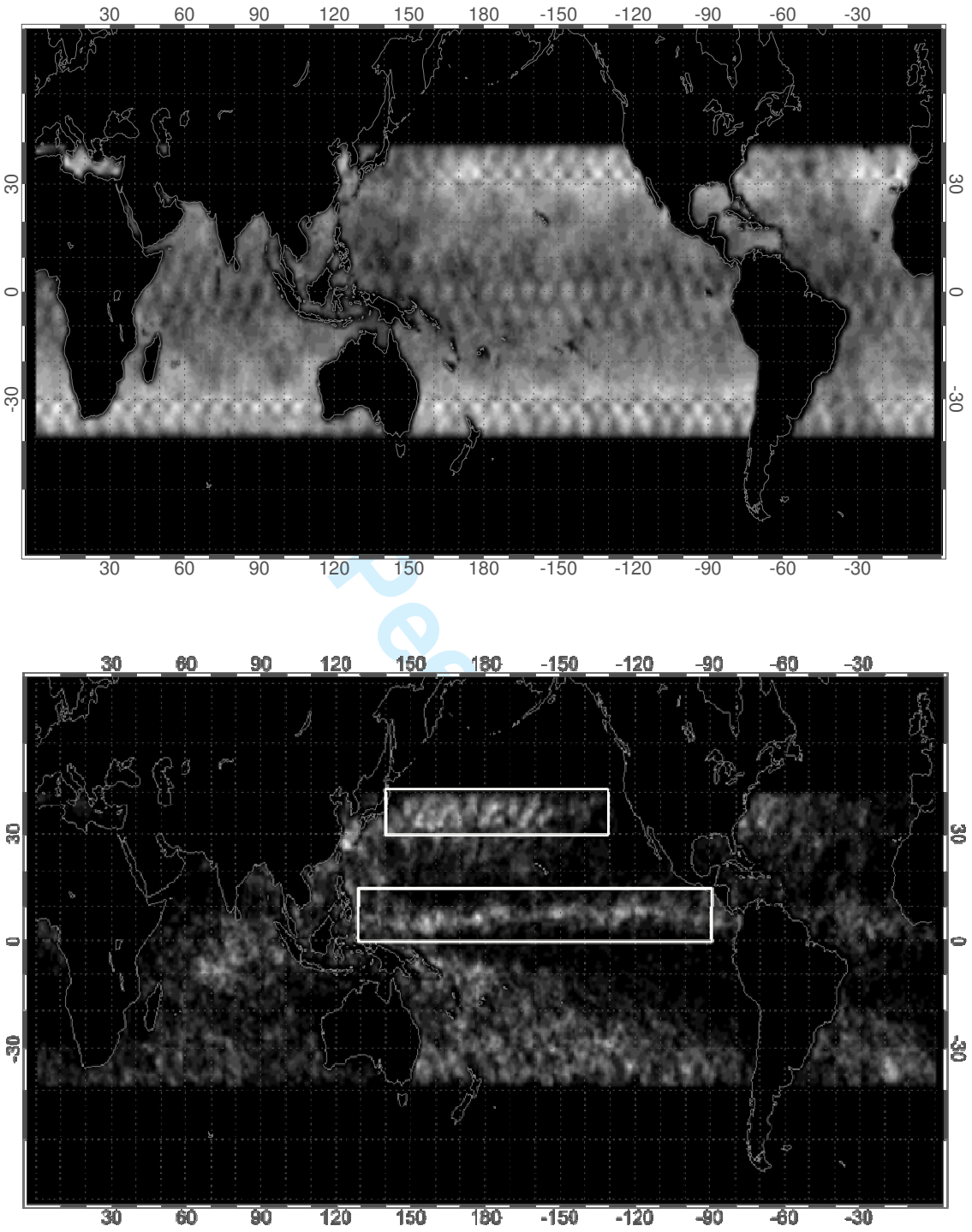

Fig. 2. Spatial distribution of the ASCAT-ECMWF-TMI collocations on a global map, both for rain free conditions (top) and for rainy conditions (bottom). A total of 5.9 (0.5) million collocations are represented in the top (bottom) panel in a 1° x 1° boxes, ranging from no collocations (black) to the maximum number (bright white). Note that two regions of interest are highlighted: the Pacific Inter Tropical Convergence Zone (ITCZ) and the Extratropical (North) Pacific area.

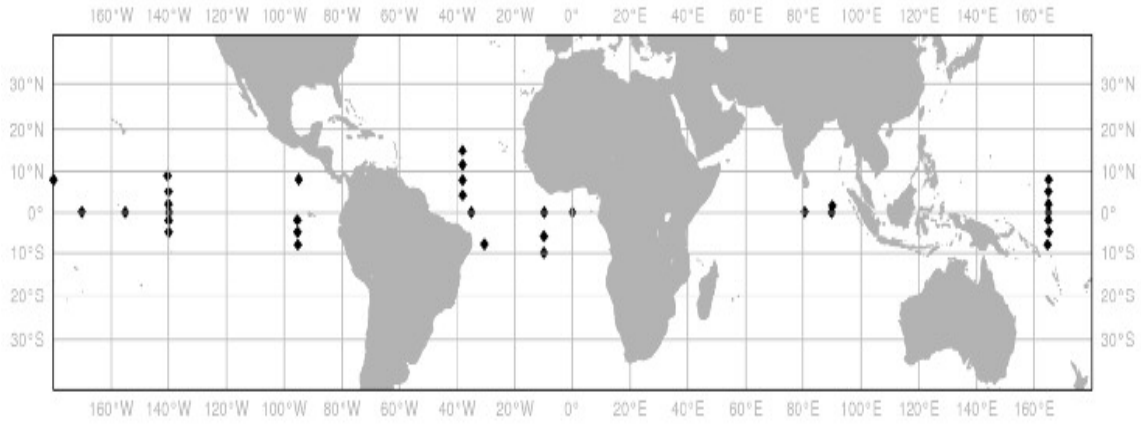

Fig. 3. Geographical location of the tropical moored buoys used.

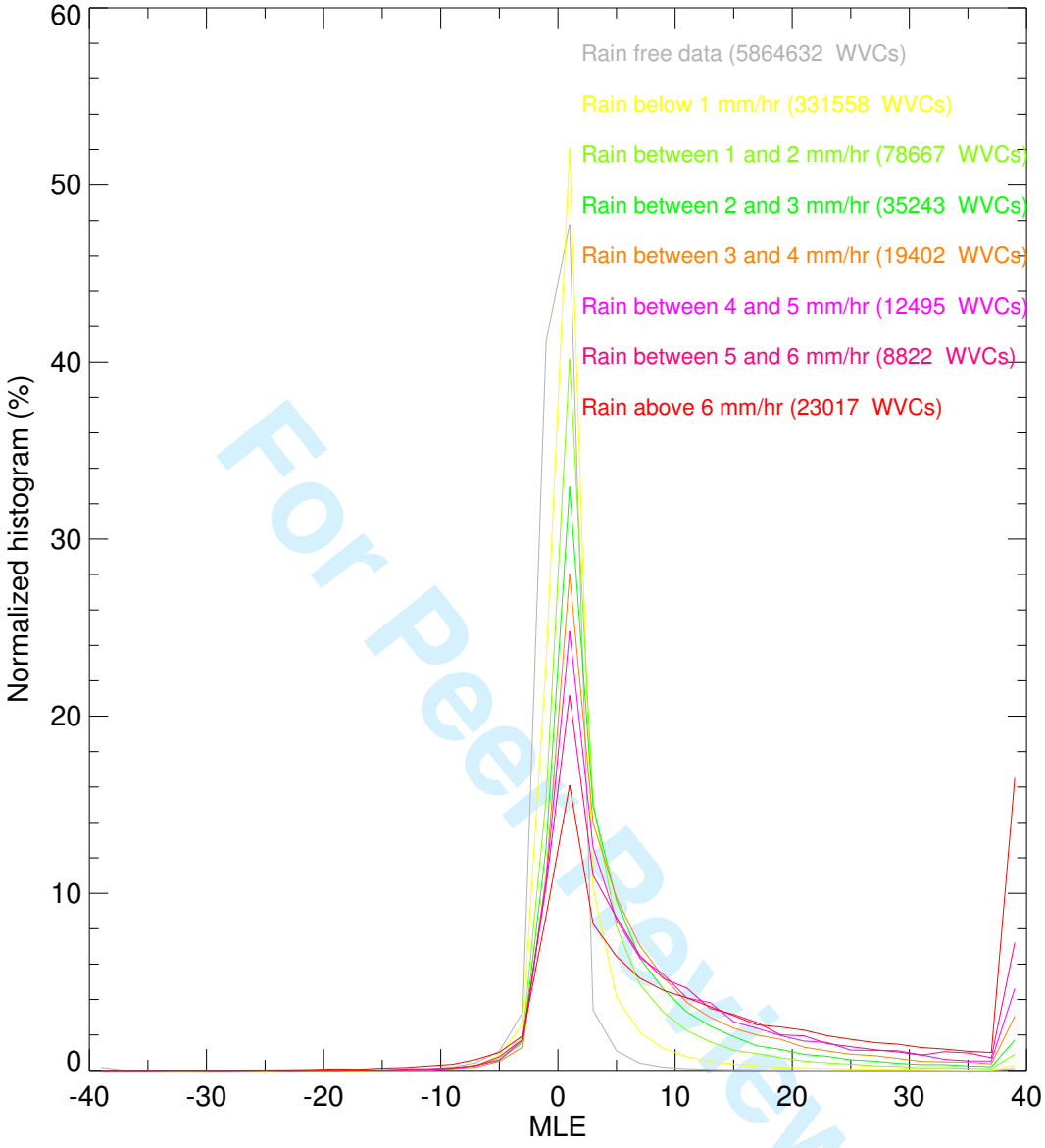

Fig. 4. MLE histogram for different rain rate (RR) intervals. Note that every coloured line corresponds to a different RR interval (see legend). The number of WVCs for each histogram is also provided in the legend.

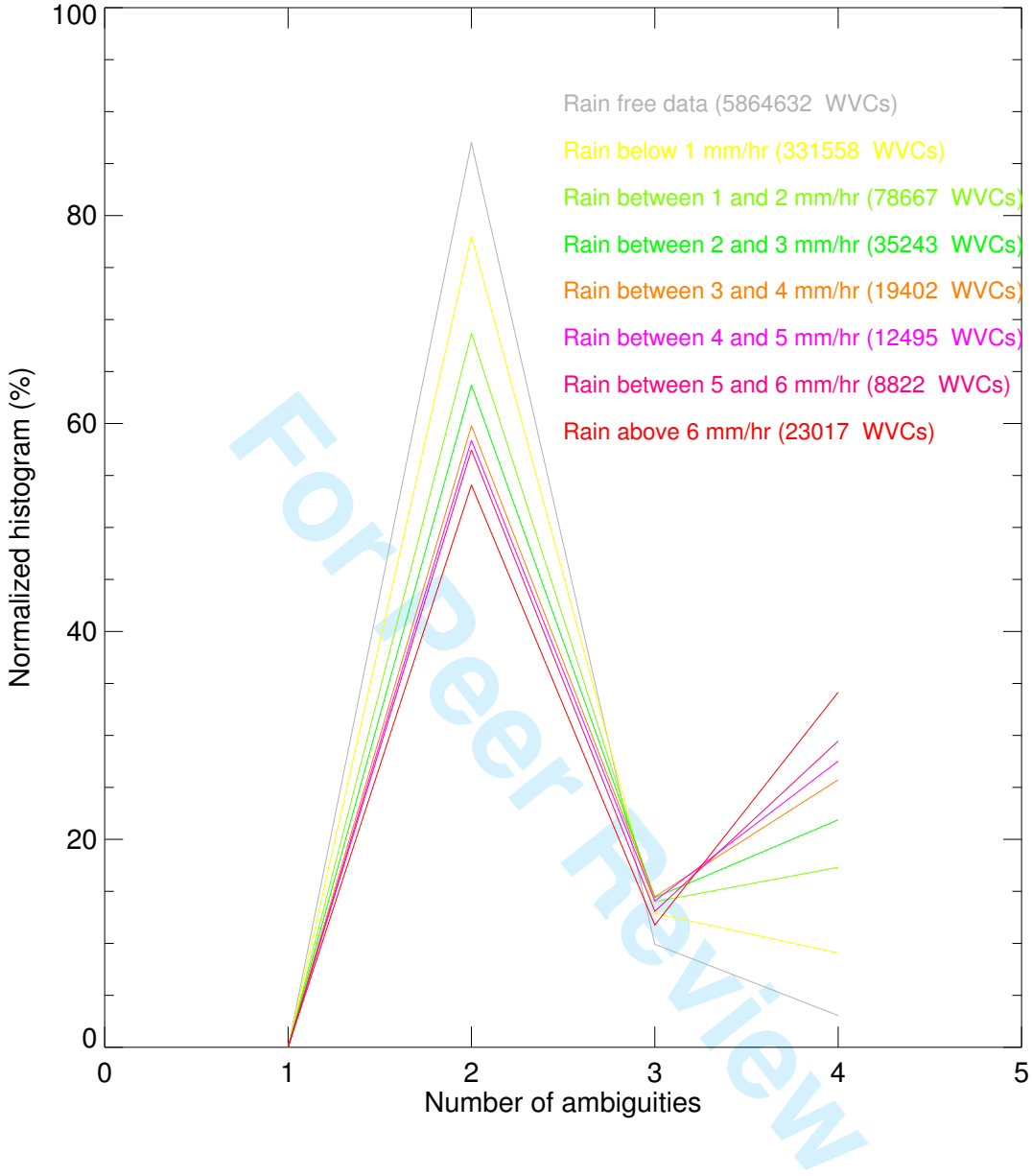

Fig. 5. Number of ASCAT retrieved wind solutions (ambiguities) for different rain rate (RR) intervals (see legend).

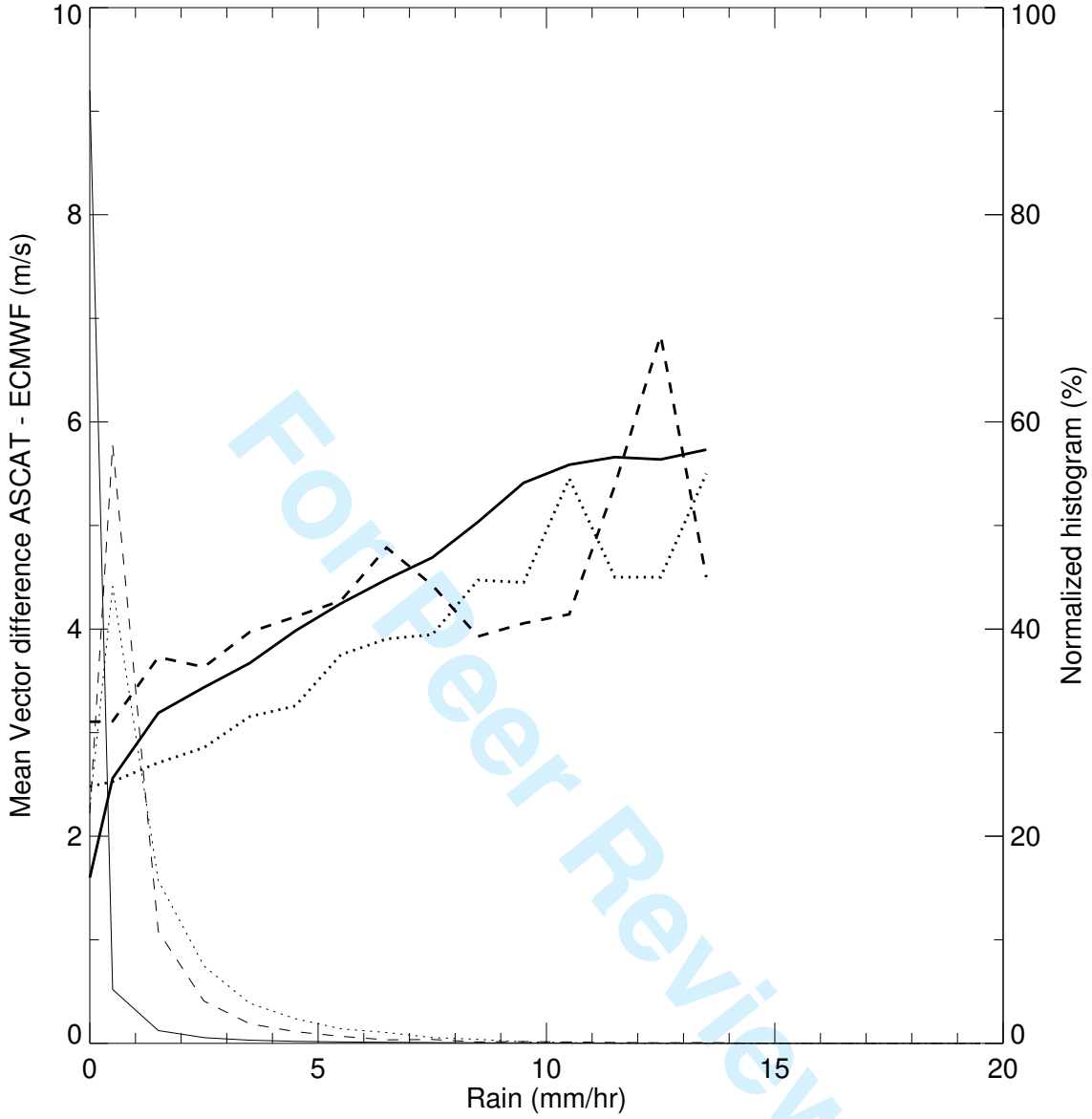

Fig. 6. Mean vector root-mean-square (VRMS) difference between ASCAT and ECMWF winds (thick lines) and percentage of data (thin lines) as a function of TMI rain rate (bins of 1 mm/hr), for three different geographical regions: global (solid), the ITCZ Pacific region (dotted) and the Extratropical Pacific (dashed).

a)

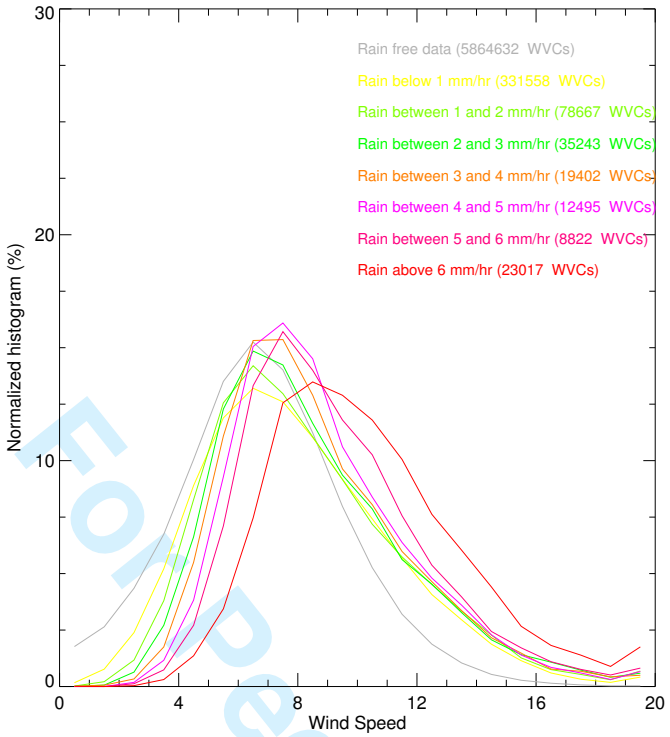

b)

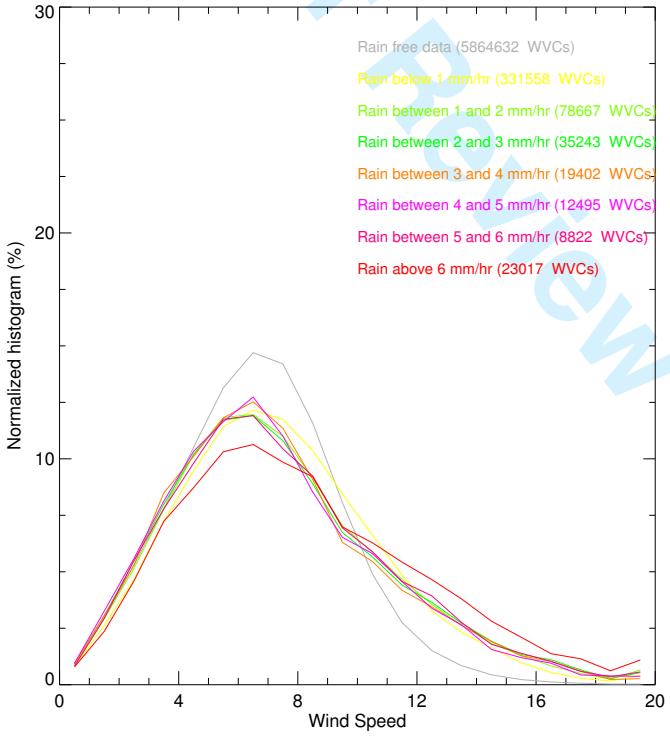

Fig. 7. Global wind speed histograms of both ASCAT (a) and ECMWF (b) winds for different TMI-derived RR intervals (see legend).

a)

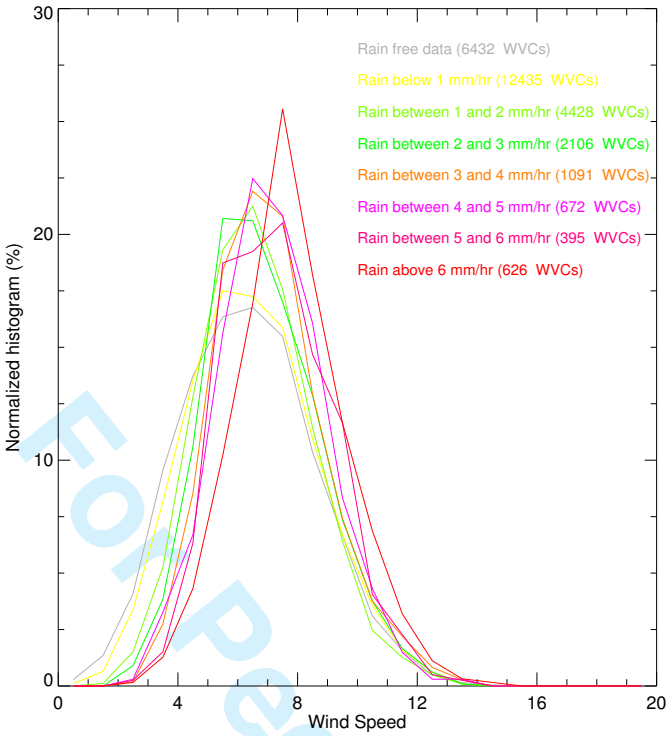

b)

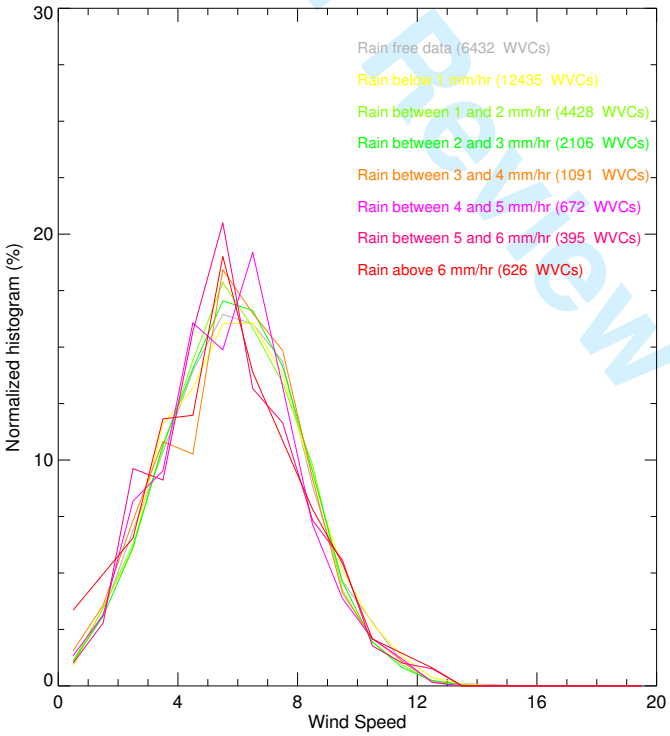

Fig. 8. Same as Fig. 7 but for the ITCZ Pacific region.

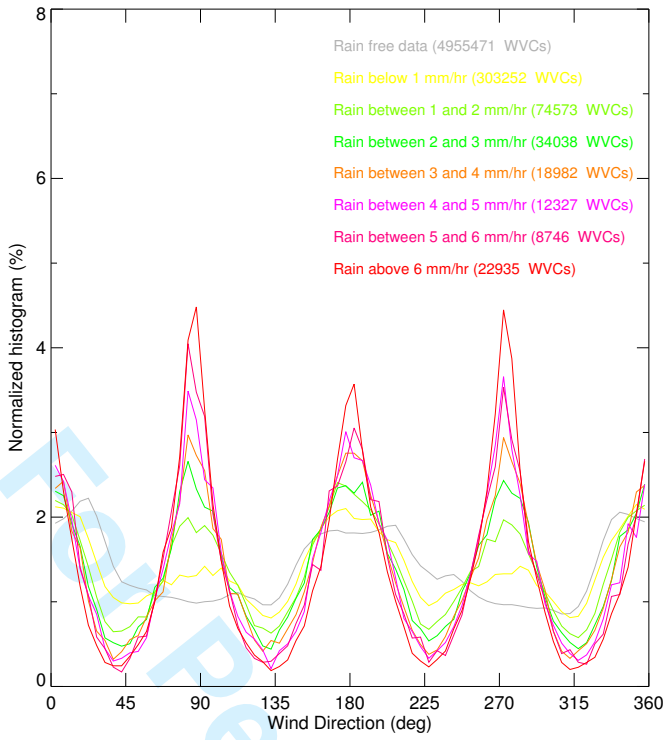

a)

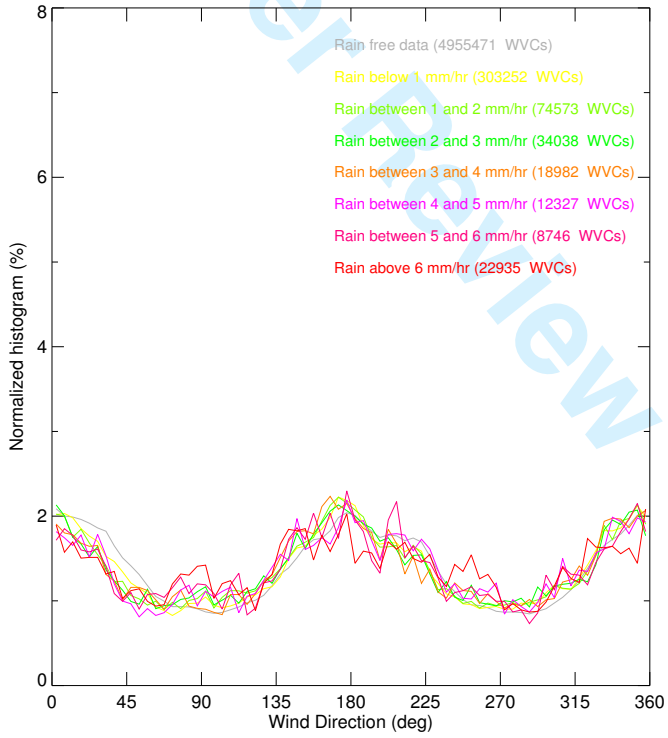

b)

Fig. 9. Histogram of ASCAT (a) and ECMWF (b) wind direction relative to the ASCAT mid antenna beam (e.g., 0° corresponds to wind blowing towards the mid beam), for different RR intervals (see legend). Note that only WVCs with retrieved wind speed above 4 m/s are used.

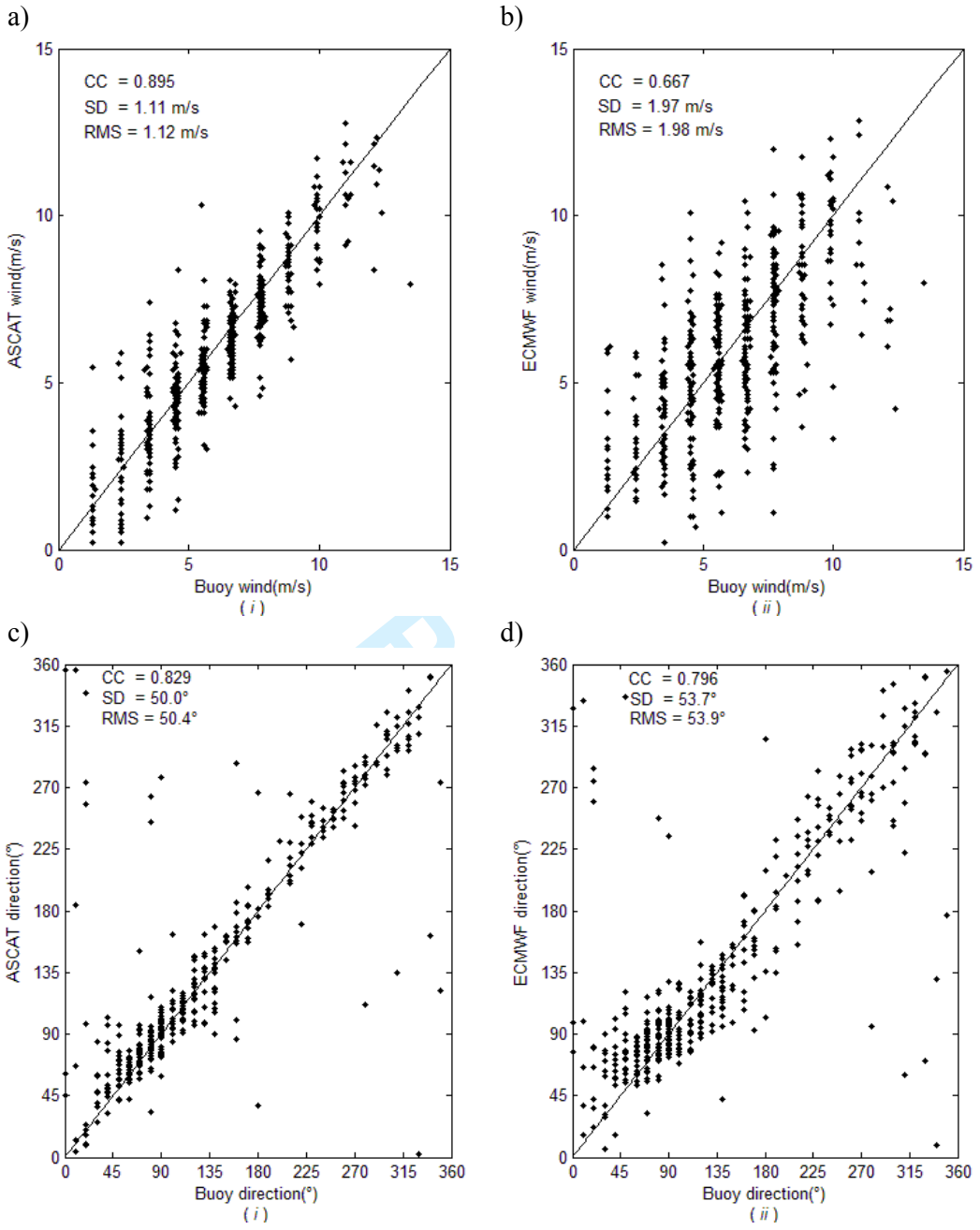

Fig 10. Scatter plots of ASCAT versus buoy (left) and ECMWF versus buoy (right) for wind speed (top) and wind direction (bottom) on rainy days, but without rain within an hour of the ASCAT overpass [C3]. Note that only buoy winds above 4 m/s are used in the wind direction plots. The legend shows the correlation coefficient (CC), the standard deviation (SD) and the RMS difference.

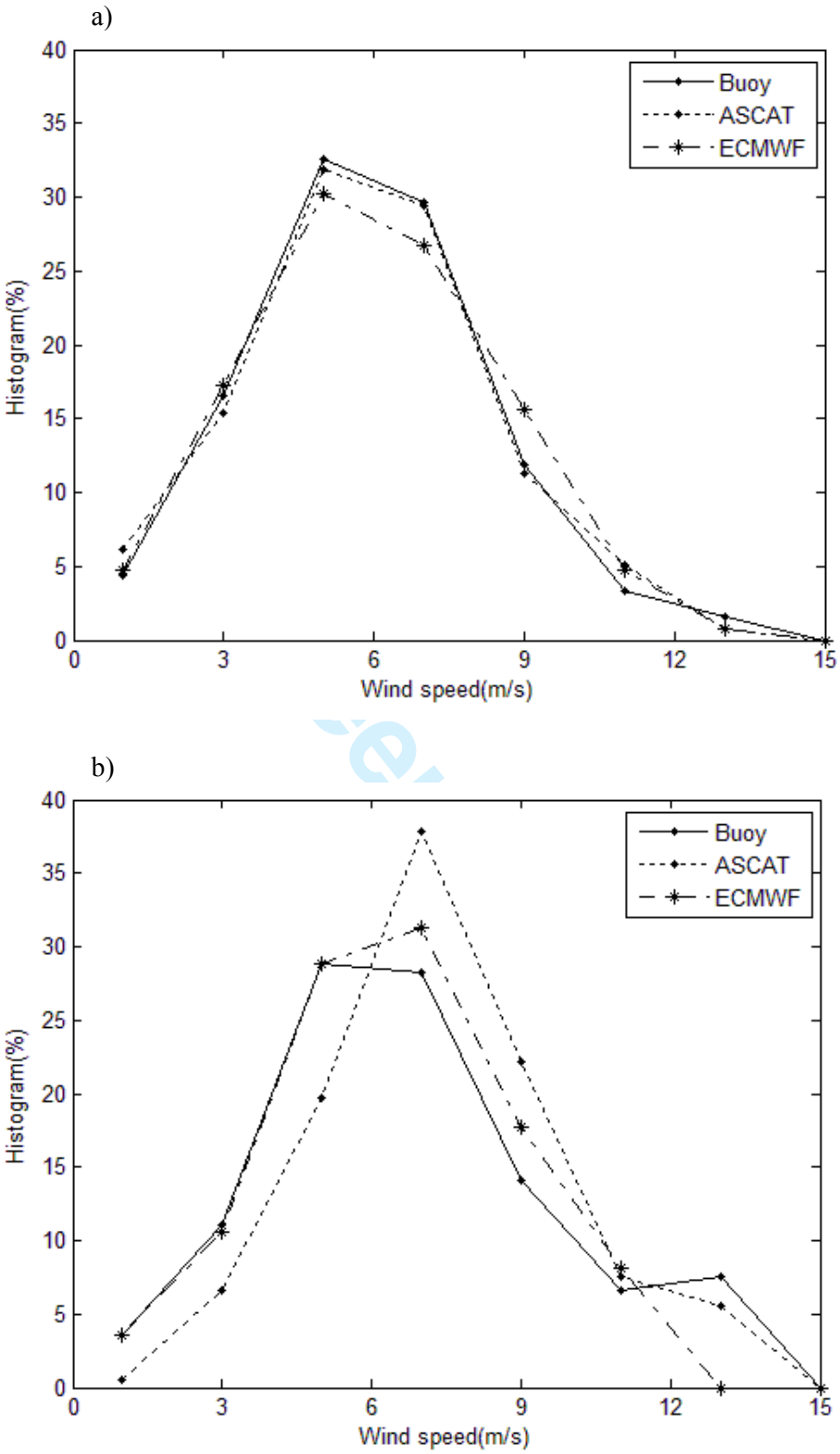

Fig. 11. Histograms of buoy (solid), ASCAT (dotted) and ECMWF (dashed) wind speeds for C3 (a) and C4 (b). Due to the small number of collocations, the binning is set to 2 m/s.

a)

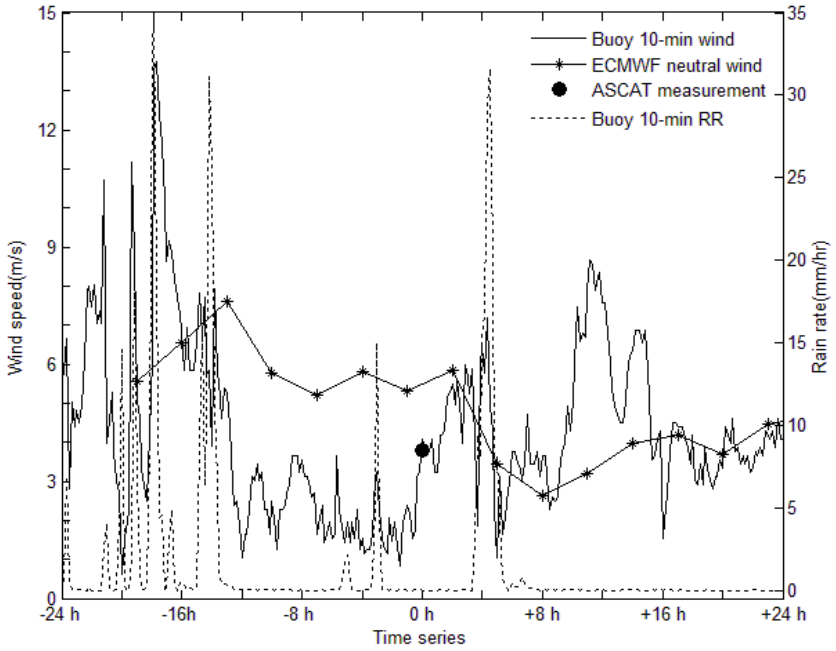

b)

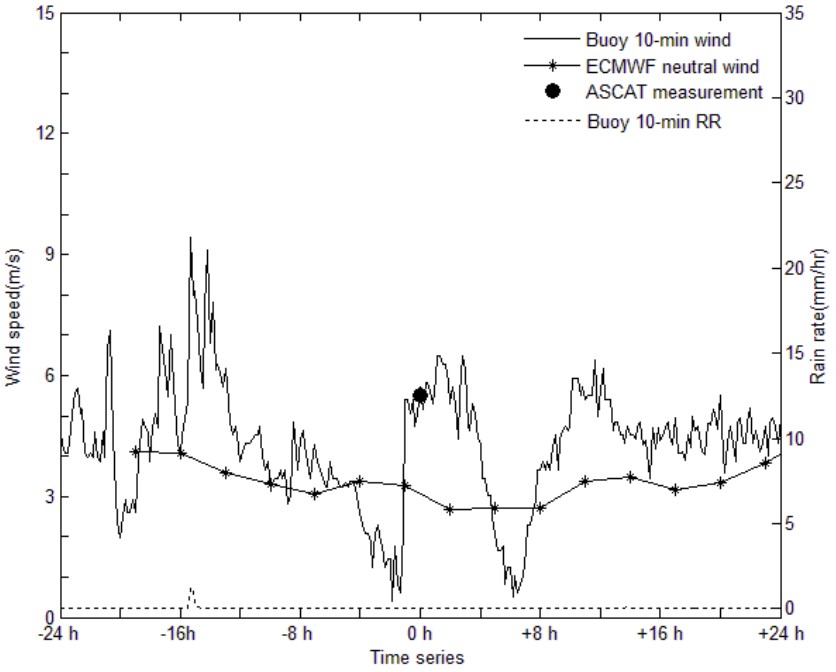

Fig. 12. Time series of buoy winds and rain, and ECMWF wind forecasts for the period of ±24 hours of the ASCAT satellite overpass (see legend). The black circle represents the ASCAT retrieved wind speed. The first time series (a) corresponds to buoy 52003 [8°S, 165°E] and is centered on August 10 2007 at 22:00 UTC. The second time series (b) corresponds to buoy 52007 [5°N, 165°E] and is centered on July 5 2007 at 10:00 UTC.

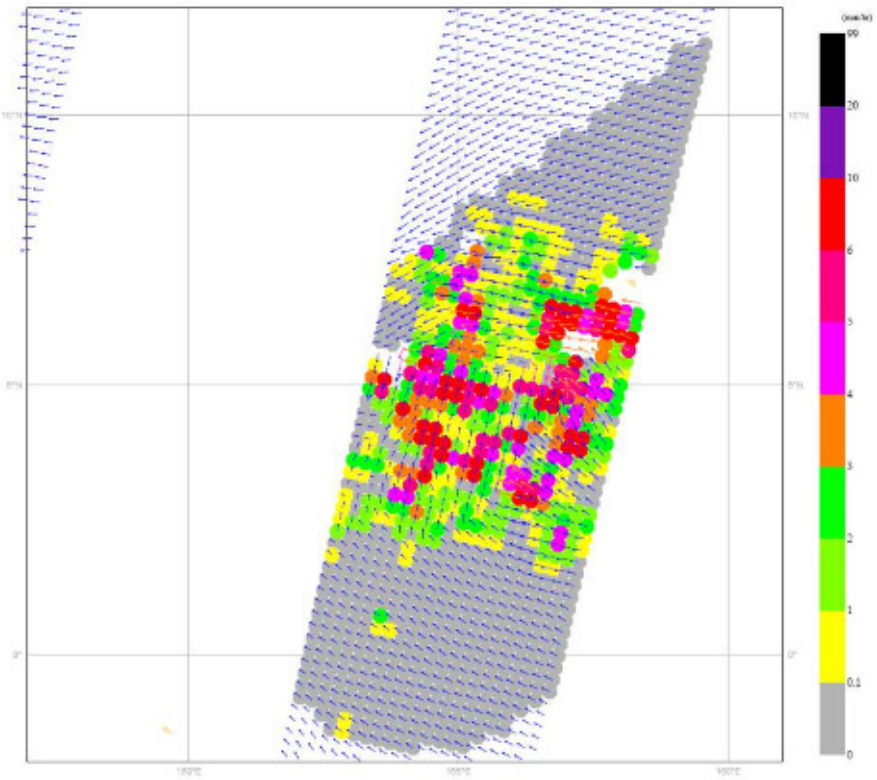

Fig. 13. Map of collocated ASCAT-TMI data. ASCAT wind arrows, where blue corresponds to QC-accepted WVCs and yellow/orange to QC-rejected WVCs. The coloured areas superimposed correspond to different TMI rain rates (see legend). The acquisition date was October 14 2008 at 22:45 UTC.

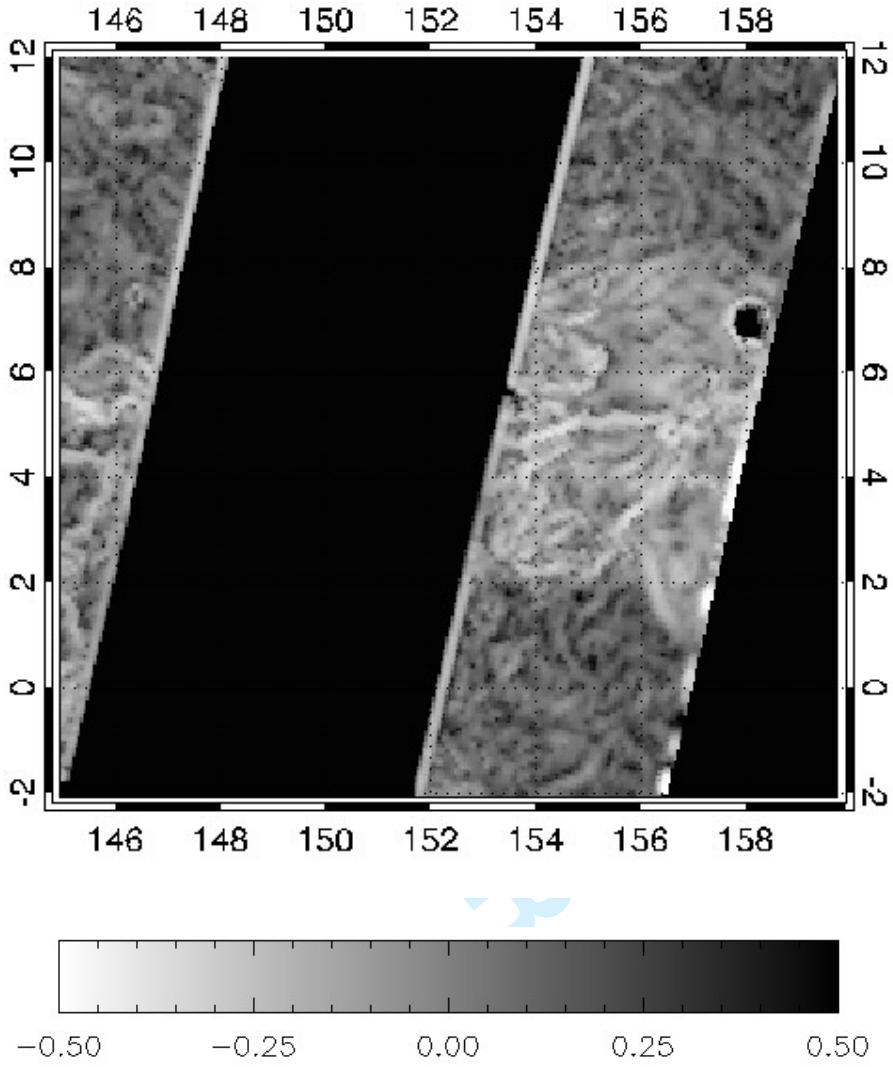

Fig. 14. Singularity map of the ASCAT retrieved wind field shown in Fig. 9. The map is constructed as the minimum exponents of the singularity maps associated to the U and V wind components.

Biographies

Marcos Portabella was born on October 14, 1970 in Spain. He received the B.Sc. degree in Physics in 1994 from the University of Barcelona, Spain; the M.Sc. in Remote Sensing in 1995 from the Institute of Space Studies of Catalonia, Spain; and the Ph.D. degree in Physics in 2002, from the University of Barcelona, Spain.

He is currently with the Unidad de Tecnología Marina (UTM – CSIC), Barcelona, Spain, working on satellite remote sensing. In particular, he is involved in scatterometry and L-band radiometry.

Ad Stoffelen was born on Feb. 25, 1962, in The Netherlands. He received his M.Sc. degree in physics from the Technical University of Eindhoven, The

Netherlands, in 1987 and his Ph.D in Meteorology on scatterometry at the University of Utrecht, the Netherlands.

He is working at KNMI and responsible for the ASCAT wind products. He is also deeply involved in the European Space Agency ADM-Aeolus Doppler Wind Lidar mission.

Wenming Lin was born on April 22, 1984 in China. He received his B.Sc. degree in Engineering in 2006 from Wuhan University, China, and his Ph.D. in Engineering in 2011 at the Center for Space Science and Applied Research, Chinese Academy of Sciences. He is currently a postdoctoral researcher at the Institute of Marine Sciences (ICM – CSIC) in Barcelona (Spain) and working on the scatterometer wind quality control.

Antonio Turiel was born on May 1, 1970 in Spain. He received his B. Sc in Physics in 1993, his B.Sc. in Mathematics in 1994 and his Ph.D. in Theoretical Physics in 1998, all three from the Autonomous University of Madrid.

He is currently working in the Department of Physical Oceanography at the Institute of Marine Sciences of CSIC in Barcelona. His research topics include signal and image processing applied to remote sensing of the oceans, marine turbulence at mesoscale and ocean circulation at different scales.

Anton Verhoef was born on Dec 10, 1964 in The Netherlands. He received his M.Sc. degree in physics from the Rijksuniversiteit Groningen, The Netherlands in 1989 and his Ph.D in Solid State Physics at the Rijksuniversiteit Groiningen in 1994.

He is currently with the Royal Netherlands Meteorological Institute (KNMI) and working on scatterometry processing software development, data validation, quality monitoring and user services.

Jeroen Verspeek was born on July 2, 1962, in The Netherlands. He received his M.Sc. degree in physics from the Technical University of Eindhoven, Eindhoven, The Netherlands, in 1988.

He is currently with the Royal Netherlands Meteorological Institute (KNMI), De Bilt, The Netherlands, and is working on scatterometer data interpretation, inversion, calibration, validation and quality monitoring.

Joaquim Ballabrera was born on March 30, 1966 in Barcelona. He received a B.Sc. degree in 1991 from the University of Barcelona. His Dyplôme d'Études Avancées (DEA) and Ph.D. degree in Geophysics are both from the University Joseph Fourier, Grenoble.

He is currently with the Unitat the Tecnologia Marina (UTM - CSIC), Barcelona, working on numerical modelling, data assimilation, and remote sensing.